Molecular Therapy
Nucleic Acids
Original Article

MicroRNA-dependent inhibition of WEE1 controls cancer stem-like characteristics and malignant behavior in ovarian cancer

Jin Gu Cho,[1,2,10] Sung-wook Kim,[3,10] Aram Lee,[1,2,10] Ha-neul Jeong,[1,10] Eunsik Yun,[1] Jihea Choi,[1] Su Jin Jeong,[4] Woochul Chang,[5] Sumin Oh,[1,2] Kyung Hyun Yoo,[1,2] Jung Bok Lee,[1,2] Sukjoon Yoon,[1,2] Myeong-Sok Lee,[1,2] Jong Hoon Park,[1,2] Min Hyung Jung,[3] So-Woon Kim,[6] Ki Hyung Kim,[7] Dong Soo Suh,[7] Kyung Un Choi,[8] Jungmin Choi,[9] Jongmin Kim,[1,2] and Byung Su Kwon[3]

[1]Division of Biological Sciences, Sookmyung Women's University, Seoul 04310, Korea; [2]Research Institute for Women's Health, Sookmyung Women's University, Seoul 04310, Korea; [3]Department of Obstetrics and Gynecology, School of Medicine, Kyung Hee University Medical Center, Kyung Hee University, Seoul 02447, Korea; [4]Kyung Hee University Medical Center, Medical Science Research Institute, Statistics Support Part, Seoul 02447, Korea; [5]Department of Biology Education, College of Education, Pusan National University, Busan 46241, Korea; [6]Department of Pathology, Kyung Hee University Hospital, Kyung Hee University College of Medicine, Seoul 02447, Korea; [7]Department of Obstetrics and Gynecology, Pusan National University School of Medicine, Biomedical Research Institute, Pusan National University Hospital, Pusan 49241, Korea; [8]Department of Pathology, Pusan National University Hospital, Busan National University School of Medicine, Busan 49241, Korea; [9]Department of Biomedical Sciences, Korea University College of Medicine, Seoul 02841, Korea

Cancer stem-like cells (CSCs) have been suggested to be responsible for chemoresistance and tumor recurrence owing to their self-renewal capacity and differentiation potential. Although WEE1 is a strong candidate target for anticancer therapies, its role in ovarian CSCs is yet to be elucidated. Here, we show that WEE1 plays a key role in regulating CSC properties and tumor resistance to carboplatin via a microRNA-dependent mechanism. We found that WEE1 expression is upregulated in ovarian cancer spheroids because of the decreased expression of miR-424 and miR-503, which directly target WEE1. The overexpression of miR-424/503 suppressed CSC activity by inhibiting WEE1 expression, but this effect was reversed on the restoration of WEE1 expression. Furthermore, we demonstrated that NANOG modulates the miR-424/503-WEE1 axis that regulates the properties of CSCs. We also demonstrated the pharmacological restoration of the NANOG-miR-424/503-WEE1 axis and attenuation of ovarian CSC characteristics in response to atorvastatin treatment. Lastly, miR-424/503-mediated WEE1 inhibition re-sensitized chemoresistant ovarian cancer cells to carboplatin. Additionally, combined treatment with atorvastatin and carboplatin synergistically reduced tumor growth, chemoresistance, and peritoneal seeding in the intraperitoneal mouse models of ovarian cancer. We identified a novel NANOG-miR-424/503-WEE1 pathway for regulating ovarian CSCs, which has potential therapeutic utility in ovarian cancer treatment.

INTRODUCTION

Epithelial ovarian cancer is the most fatal type of gynecological tumor, and the mortality rate of this disease has not shown any significant reduction over the last 30 years.[1,2] Most patients exhibit high responsiveness to current platinum-based chemotherapies; however, in terms of long-term survival and cure rates, these treatments are unsatisfactory. This is primarily due to the progressive acquisition of treatment resistance and development of the disease into a recurrent form.[3–6] In addition, ovarian cancer exhibits lethal metastatic behavior. This behavior is attributed to a specific subpopulation of cancer cells, namely, ovarian cancer stem-like cells (CSCs), which are closely associated with ovarian cancer chemoresistance, recurrence, and metastasis.[4–8] Therefore, ovarian CSC-targeting strategies are fundamental for overcoming the limitations of the current therapies against ovarian cancer.

CSCs have been shown to elicit an enhanced DNA damage response (DDR), which facilitates radiation resistance and chemoresistance.[9–11] For example, $CD133^+$ glioma stem cells induced radiation resistance in gliomas through the activation of the DNA damage checkpoint response, and the resistance could be reversed by treatment with debromohymenialdisine, an inhibitor of the checkpoint kinases Chk1 and Chk2.[10] In addition, the inhibition of Chk1 sensitized pancreatic CSCs to chemotherapeutics.[11] These findings strongly suggest that targeting cell-cycle regulators in CSCs could be a promising

Received 9 April 2022; accepted 17 August 2022;
https://doi.org/10.1016/j.omtn.2022.08.028.

[10]These authors contributed equally

Correspondence: Jongmin Kim, Division of Biological Sciences, Sookmyung Women's University, Seoul 04310, Korea.
E-mail: jkim@sookmyung.ac.kr
Correspondence: Byung Su Kwon, Department of Obstetrics and Gynecology, School of Medicine, Kyung Hee University Medical Center, Kyung Hee University, Seoul 02447, Korea.
E-mail: kbsgyonco@naver.com

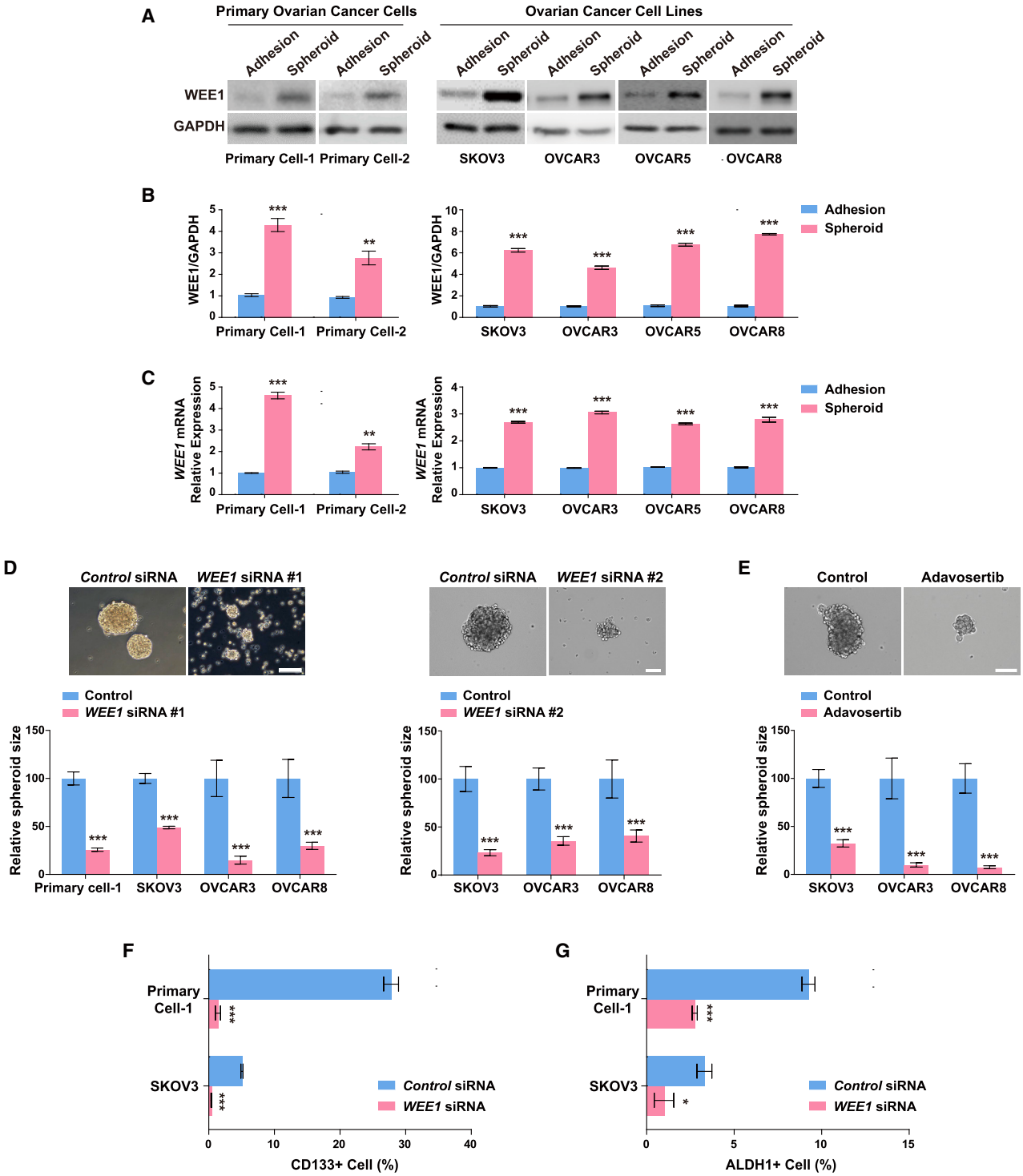

Figure 1. WEE1 upregulation in ovarian cancer spheroids regulates cancer stem cell-like properties

Comparison of WEE1 protein (A and B) and mRNA (C) expression in adherent and spheroid cultures of various ovarian cancer cell lines and primary ovarian cancer cells. (D) Representative images of spheroids after *WEE1* knockdown in SKOV3 cells. The sizes of spheroids in primary ovarian tumor cells and various ovarian cancer cell lines (SKOV3, OVACAR3, and OVCAR8) after *WEE1* knockdown. Scale bars: 100 μm. (E) Representative images of SKOV3 spheroids after treatment with 200 nM adavosertib.

(legend continued on next page)

therapeutic strategy for CSC eradication; therefore, it is critical to determine whether cell-cycle regulators play a key role in regulating ovarian CSCs.

WEE1, a protein kinase, is one of the key factors that regulate the G2-M cell-cycle checkpoint. In particular, the role of WEE1 is crucial in p53 mutant cancer cells, in which the G1 checkpoint fails to arrest cell-cycle progression in response to DNA damage, unlike in normal cells. These cancer cells primarily rely on the G2 checkpoint for DNA damage repair, which is the underlying mechanism that allows cancer cells to overcome the cytotoxicity caused by DNA-damaging reagents. In addition, WEE1 upregulation is associated with a short relapse-free period and poor overall survival (OS) in patients with various types of cancer, including glioblastoma, hepatocellular carcinoma, and breast and ovarian cancers.[12–16] Therefore, therapeutic strategies targeting WEE1 and small molecule inhibitors of the G2 checkpoint have been developed to sensitize cancer cells to conventional DNA-damaging agents and radiotherapy; this would help induce cancer-specific synthetic lethality.[17,18] However, even though studies have demonstrated that WEE1 is a strong candidate target, its role in ovarian cancer progression and stemness has not yet been elucidated.

MicroRNAs (miRNAs) are small non-coding RNAs comprising 21–22 nucleotides. miRNAs post-transcriptionally regulate gene expression by binding to the seed sequence at the 3′ untranslated region (UTR) of the target mRNAs and either inhibit their translation or induce their decay. Each miRNA targets a dozen to a hundred mRNAs because of the imperfect base pairing, and a single mRNA may be regulated by multiple miRNAs.[19,20] miRNAs are extensively involved in cellular processes, including development, organogenesis, apoptosis, proliferation, and differentiation.[21] The dysregulation of miRNA expression causes the onset of several diseases; multiple miRNAs are known to be differentially regulated in diverse cancer types, including breast, colon, pancreatic, and ovarian cancer.[22–27] Recent studies have shown that miRNAs regulate cancer stem cell-like properties, such as self-renewal, tumorigenicity, and drug resistance.[28–30]

Statins are competitive inhibitors of 3-hydroxy-3-methyl-glutaryl (HMG)-CoA reductase. They are commonly used as cholesterol-lowering drugs and effectively reduce cardiovascular disease risk.[31] Interestingly, accumulating evidence suggests that statins also present activity against various types of cancer and improve the effectiveness of chemotherapeutic agents.[31,32] Furthermore, statins regulate the expression of various cell-cycle regulatory genes and miRNAs in several types of cancer cell.[33,34] However, their effect on ovarian CSC regulation and the mechanism underlying the statin-mediated regulation of WEE1 and miRNAs is largely unknown.

In the present study, we sought to define the role of WEE1 in regulating the cancer stem cell-like properties of ovarian cancer cells.

RESULTS

WEE1 upregulation in ovarian cancer spheroids regulates cancer stem cell-like characteristics

To investigate whether WEE1 controls the cancer stem cell-like characteristics in ovarian cancer, we compared the WEE1 expression levels in three-dimensional suspension cultures with those in two-dimensional adherent cultures of multiple ovarian cancer cell lines and primary ovarian tumor cells, which are known to be enriched in CSCs.[35,36] The WEE1 mRNA and protein expression levels were increased to a considerable extent in the three-dimensional suspension cultures of epithelial ovarian cancer cell lines (SKOV3, OVCAR3, OVCAR5, and OVCAR8) and primary ovarian cancer cells, which indicated the involvement of WEE1 in the formation of ovarian cancer cell spheroids (Figures 1A–1C). To determine whether WEE1 is involved in the regulation of cancer stem cell-like characteristics, we tested the effect of *WEE1* knockdown (Figures S1A and S1B) on spheroid formation in primary ovarian cancer cells and epithelial ovarian cancer cell lines (SKOV3, OVCAR3, and OVCAR8). *WEE1* knockdown significantly suppressed spheroid formation (Figure 1D), as did adavosertib, a WEE1 inhibitor, in SKOV3, OVCAR3, and OVCAR8 cells (Figure 1E). A striking feature of ovarian cancer spheroids is the enrichment of the population with CSC markers such as CD133 and ALDH1.[37–39] The $CD133^+$ population in primary ovarian cancer cells and SKOV3 cells was significantly decreased on *WEE1* knockdown in spheroids (Figure 1F). Consistently, the percentage of $ALDH1^+$ cells decreased significantly in the *WEE1*-knockdown spheroids compared with control spheroids (Figure 1G). These results provide evidence that WEE1 inhibition decreases the abundance of $CD133^+$ and $ALDH1^+$ cells and suppresses spheroid formation in ovarian cancer cells.

WEE1 upregulation in ovarian cancer spheroids is associated with miR-424 and miR-503 suppression

Given the involvement of WEE1 expression in the promotion of cancer stem cell-like characteristics in ovarian cancer spheroids, we investigated the mechanism underlying the upregulation of WEE1 expression in spheroids. Accumulating data suggest the important role of miRNA-mediated regulation in different cellular contexts, such as in laryngeal carcinoma,[40] melanoma,[41] and glioma.[42] We hypothesized that WEE1 upregulation in ovarian cancer spheroids might be mediated by miRNAs that affect the stability of *WEE1* mRNA. To test this hypothesis, we first examined whether the knockdown of argonaute 2 (AGO2), a key component of the RNA-induced silencing complex, affected WEE1 expression in SKOV3 cells. *AGO2* knockdown significantly increased WEE1 expression, indicating that WEE1 expression is subject to miRNA-mediated regulation in ovarian cancer cells (Figures 2A and 2B).

Next, we attempted to identify the specific miRNAs potentially involved in the regulation of WEE1 expression in ovarian cancer

The sizes of the spheroids formed from SKOV3, OVACAR3, and OVCAR8 cells treated with 200 nM adavosertib were significantly smaller compared with the control. Scale bar: 100 μm. Fluorescence-activated cell sorting analysis of the $CD133^+$ (F) and $ALDH1^+$ (G) population in primary ovarian cancer cells and SKOV3 cells after *WEE1* knockdown. *$p < 0.05$, **$p < 0.01$, ***$p < 0.001$ for comparisons indicated by unpaired two-tailed Student's t test. Error bars, standard error of the mean.

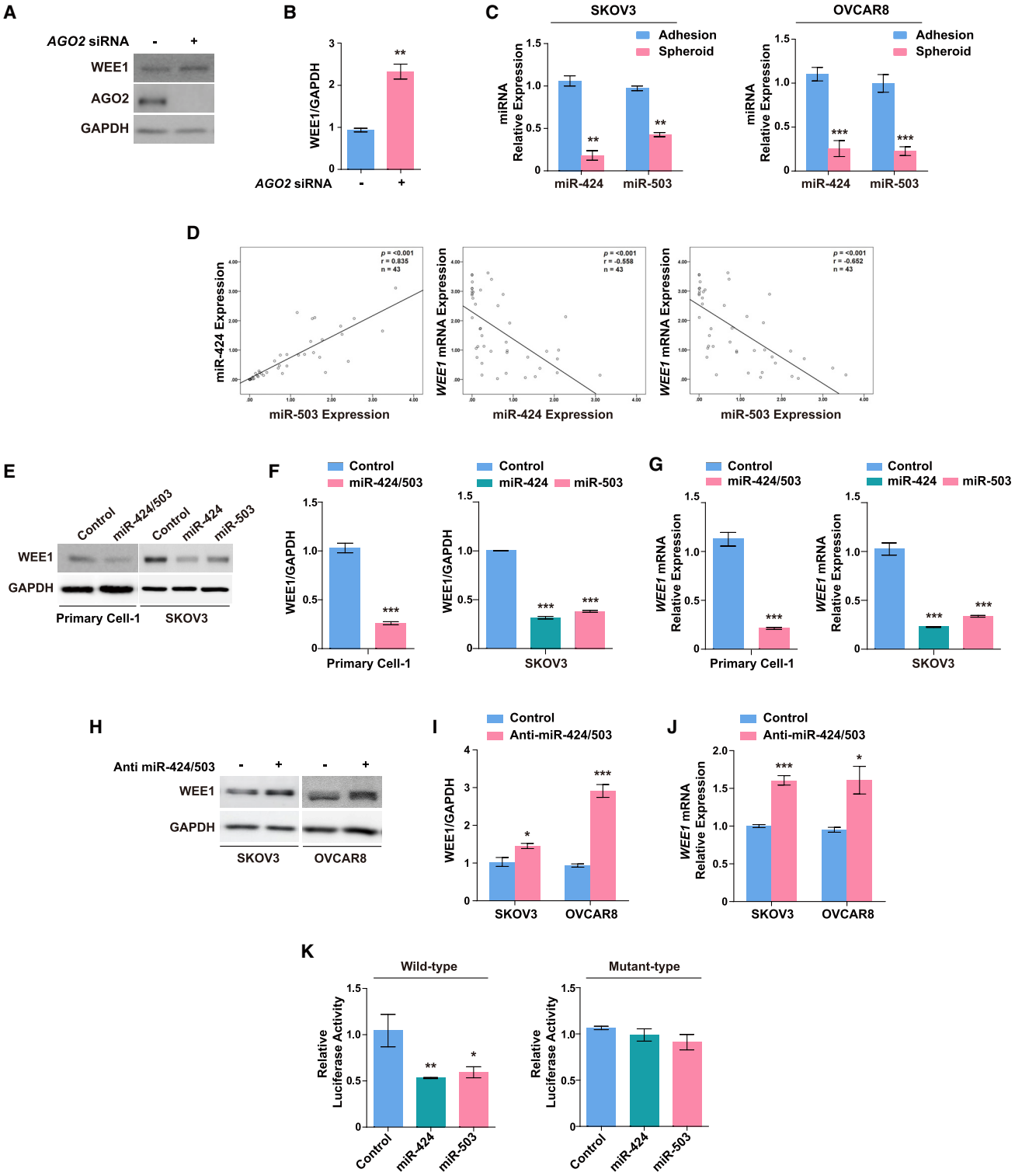

Figure 2. miR-424 and miR-503 directly target WEE1 in ovarian cancer cells

(A and B) WEE1 protein expression after *AGO2* siRNA transfection in SKOV3 cells. (C) Mature miR-424 and miR-503 expression in SKOV3 and OVCAR8 adherent cells and spheroids. (D) Linear correlation between miR-424 and miR-503 expression. Inverse correlation between *WEE1* mRNA expression and miR-424/miR-503 expression in ovarian tumor tissues. Relationships between variables were determined by the Pearson correlation coefficient. WEE1 protein (E and F) and mRNA (G) expression in response

(legend continued on next page)

spheroids. An miRNA microarray had been previously performed using ovarian cancer cell spheroids, and five differentially regulated miRNAs were identified.[43] Among these, only miR-424 was substantially downregulated in ovarian cancer spheroids,[43] and using *in silico* analysis it was predicted that miR-424 would target the 3′ UTR of WEE1 (Figure S2). We previously reported that miR-424 and miR-503 are derived from a single transcript, exhibit substantial identity in their seed sequences, and perform similar functions in different cellular contexts.[44,45] In addition, previous studies have reported miR-424 and miR-503 as tumor suppressors in several cancer types and have shown that their levels are significantly decreased in ovarian cancers.[46–48] Accordingly, we investigated whether the expression levels of both miR-424 and 503 are affected in ovarian cancer spheroids. We found a significant reduction in both miR-424 and miR-503 expression levels, suggesting their potential involvement in the upregulation of WEE1 expression in ovarian cancer spheroids (Figure 2C). To further investigate the interaction between miR-424/503 and WEE1, we measured the miR-424/503 and WEE1 levels in ovarian tumor tissues. Given that miR-424 and miR-503 are transcribed as a single transcript, there was a highly significant linear correlation between the expression levels of miR-424 and miR-503. We also found that the WEE1 levels were inversely correlated with the levels of miR-424 and miR-503 (Figure 2D). These findings were verified by analysis of publicly available ovarian cancer datasets from the National Center for Biotechnology Information (GEO: GSE30161); an inverse correlation between WEE1 levels and levels of miR-424/503 was confirmed (Figure S3A). Furthermore, Kaplan-Meier survival analysis demonstrated that a higher level of WEE1 expression was correlated with worse progression-free survival (PFS; hazard ratio [HR], 3.04; 95% CI, 1.46–6.33; $p = 0.0019$) and OS (HR, 2.93; 95% CI, 1.34–6.44; $p = 0.0053$) (Figure S3B), while a higher level of miR-424/503 expression revealed a trend in PFS (HR, 0.65; 95% CI, 0.3–1.39; $p = 0.26$) and OS (HR, 0.56; 95% CI, 0.26–1.22; $p = 0.14$) (Figure S3C). Because the data showed an inverse correlation between the levels of miR-424/503 and WEE1 in ovarian cancer spheroids and ovarian tumor tissues, we speculated that WEE1 might be a direct target of miR-424/503. To evaluate the miR-424/503-mediated regulation of WEE1 in ovarian cancer cells, we first determined the effects of miR-424/503 overexpression on WEE1 expression in primary ovarian cancer cells and SKOV3 cells. We found that miR-424/503 overexpression in both cell types led to a significant decrease in the mRNA and protein expression of WEE1 (Figures 2E–2G and S4A), whereas the inhibition of endogenous miR-424/503 upregulated WEE1 mRNA and protein expression in ovarian cancer cells (Figures 2H–2J and S4B).

To further determine whether miR-424/503 regulates WEE1 expression by binding directly to the WEE1 3′ UTR, we generated luciferase reporter constructs using the 3′ UTR sequence of WEE1. We found that miR-424 and miR-503 overexpression significantly suppressed the reporter activity, whereas this effect was completely abrogated with the mutant WEE1 3′ UTR (Figure 2K). Collectively, these findings suggested that miR-424 and miR-503 are downregulated in ovarian cancer spheroids, and WEE1 is directly targeted by miR-424 and miR-503 in ovarian cancer cells.

miR-424 and miR-503 exert tumor-suppressive effects *in vitro* and *in vivo*

To determine the functional roles of miR-424 and miR-503 in ovarian cancer cells, we first tested the effects of miR-424 and miR-503 on cell proliferation, migration, and colony formation in two-dimensional adherent cultures of multiple ovarian cancer cell lines. As shown in Figures 3A and S5A, miR-424 and miR-503 overexpression reduced the viability of adherent SKOV3, OVCAR3, OVCAR5, and OVCAR8 cells at 48 h after transfection. In addition, the results of the colony formation assay revealed the inhibition of colony formation in SKOV3 and OVCAR8 cells transfected with miR-424 or miR-503 compared with the control groups (Figures 3B and S5B). We next investigated the roles of miR-424 and miR-503 in the migration of SKOV3 cells. The overexpression of miR-424 and miR-503 significantly reduced migration in their respective groups compared with that in the controls (Figures 3C and S5C). To determine whether miR-424/503 also exert a tumor-suppressive effect *in vivo*, we established stable SKOV3 cell lines expressing miR-424 and miR-503, which showed robust miR-424 and miR-503 expression (data not shown). Nude mice bearing miR-424/503-overexpressing SKOV3 xenografts presented with fewer tumors and a markedly smaller tumor size than mice injected with control cells (Figure 3D), which further validated our *in vitro* findings that miR-424/503 exert tumor-suppressive effects. Finally, to assess the therapeutic effect of miR-424/503 overexpression on SKOV3 tumor regression, we intratumorally injected lentivirus-expressing miR-424/503 into established SKOV3-derived tumors. The tumors in the miR-424/503-expressing lentivirus group showed decreased size at day 12 compared with those in the control lentivirus group, and no significant changes were observed in body weights among the different groups (Figures 3E and S6). These data demonstrate that lentivirus-mediated overexpression of miR-424/503 is an effective therapeutic strategy for ovarian cancer.

miR-424 and miR-503 suppress cancer stem cell-like characteristics in ovarian cancer cells

On confirming that miR-424 and miR-503 directly regulate WEE1 and suppress tumor progression in ovarian cancer, we further investigated the regulative effect of miR-424 and miR-503 on the properties of CSCs. Consistent with the findings of *WEE1* knockdown, miR-424 and miR-503 overexpression markedly decreased spheroid formation, whereas the inhibition of endogenous miR-424/503 significantly increased spheroid formation (Figures 4A, 4B, S7A, and S7B). In

to the overexpression of miR-424, miR-503, or both (miR-424/503) in primary ovarian cancer cells and SKOV3 cells. (H–J) WEE1 protein and mRNA expression after transfection with anti-miR-424/503 in SKOV3 and OVCAR8 cells. (K) Targeting of the WEE1 3′ untranslated region (UTR) via miR-424 and miR-503 overexpression in SKOV3 cells. Luciferase activity data for constructs with the wild-type and mutant 3′ UTR constructs are shown. *$p < 0.05$, **$p < 0.01$, ***$p < 0.001$ compared with controls by unpaired two-tailed Student's t test or one-way analysis of variance (ANOVA) with Bonferroni's multiple comparison test. Error bars, standard error of the mean.

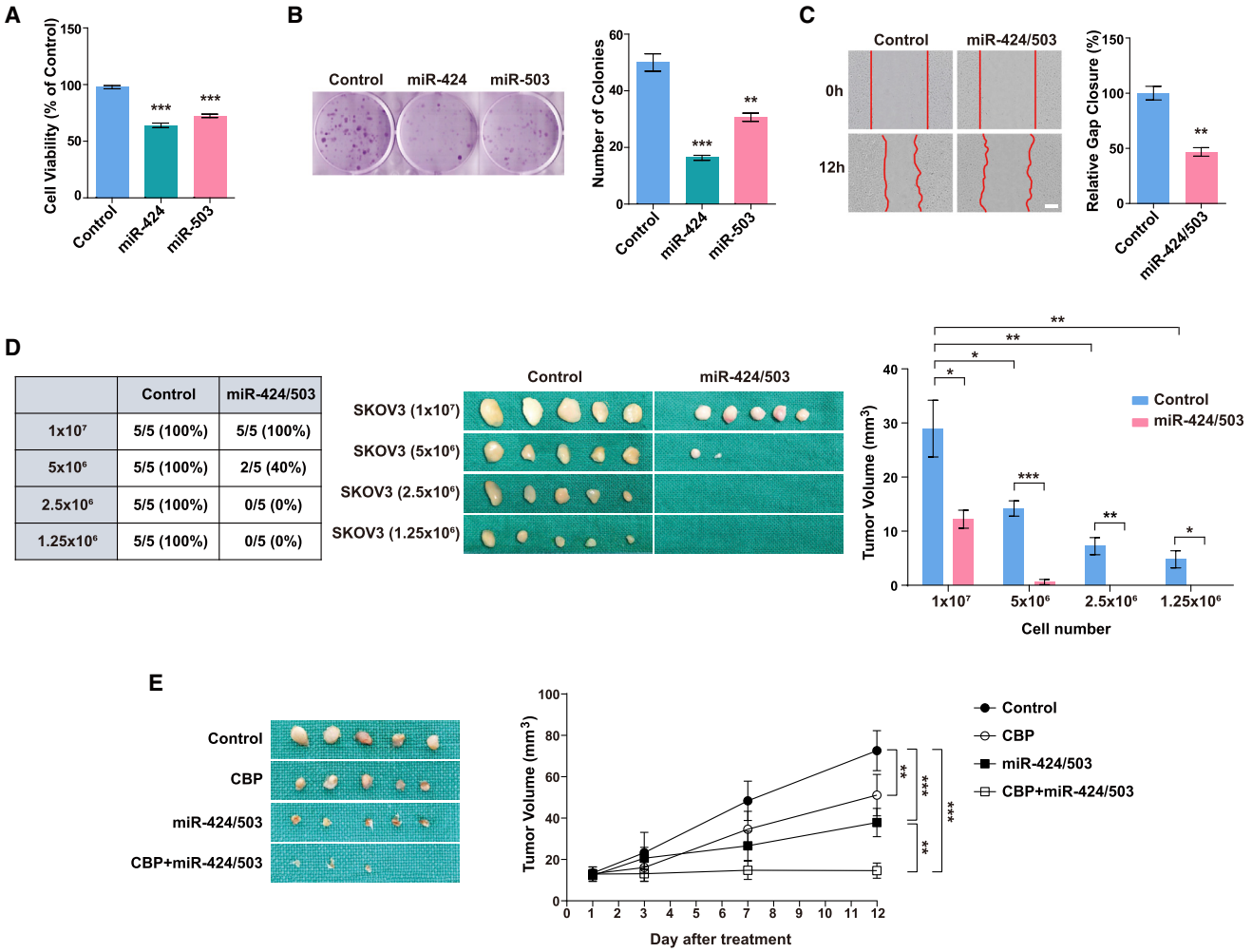

Figure 3. miR-424 and miR-503 act as tumor suppressors *in vitro* and *in vivo*

(A) Cell viability after the overexpression of miR-424 and miR-503 in adherent SKOV3 cells. (B) Colony formation was determined using crystal violet staining 14 days after the miR-424 and miR-503 overexpression in adherent SKOV3 cells. Representative images of the (C) migration assay after miR-424/503 overexpression in adherent SKOV3 cells. Scale bar: 200 μm. (D) Incidence and size of subcutaneous tumors in nude mice at 14 days after injection with control or miR-424/503-overexpressing SKOV3 cells. The graphs show significantly decreased tumor size in mice injected with miR-424/503-overexpressing cells compared with that in mice injected with control cells. *$p < 0.05$, **$p < 0.01$, ***$p < 0.001$ compared with controls by unpaired two-tailed Student's t test or two-way ANOVA with Bonferroni's multiple comparison test. Error bars, standard error of the mean. (E) Therapeutic efficacy of lentivirus-expressing miR-424/503 on established xenografts compared with the Virus Scramble xenografts. **$p < 0.01$, ***$p < 0.001$ by mixed model for repeated data with Bonferroni's multiple comparison test.

addition, miR-424 and miR-503 decreased the viability of spheroid cells (Figures 4C, S7C, and S7D), as observed in monolayers. Moreover, miR-424 and miR-503 overexpression significantly decreased the percentage of ALDH1$^+$ and CD133$^+$ populations in primary ovarian tumor cells and SKOV3 cells (Figures 4D and 4E). Lastly, we examined whether WEE1 overexpression could reverse the effects of miR-424 and miR-503 on spheroid formation. We found that the effects of miR-424 and miR-503 overexpression were abrogated in response to concurrent WEE1 overexpression. As shown in Figures 4F and S8, the co-transfection of miR-424/503 and Flag-WEE1 restored the WEE1 protein level and rescued spheroid formation in ovarian cancer cells, which were initially attenuated by miR-424 and miR-503. Collectively, these data indicate that miR-424/503 overexpression can impede ovarian cancer growth and suppress tumor recurrence by inhibiting cancer stem cell-like characteristics in ovarian cancer cells.

miR-424/503 help reduce chemoresistance and suppress peritoneal seeding

Ovarian cancer spheroids display greater protection from apoptosis and higher drug resistance when treated with chemotherapeutic drugs compared with monolayer ovarian cancer cells.[49] Hence we investigated whether miR-424 and miR-503 could help overcome spheroid-related chemoresistance. The spheroid formation assay showed that spheroid formation from SKOV3 cells expressing

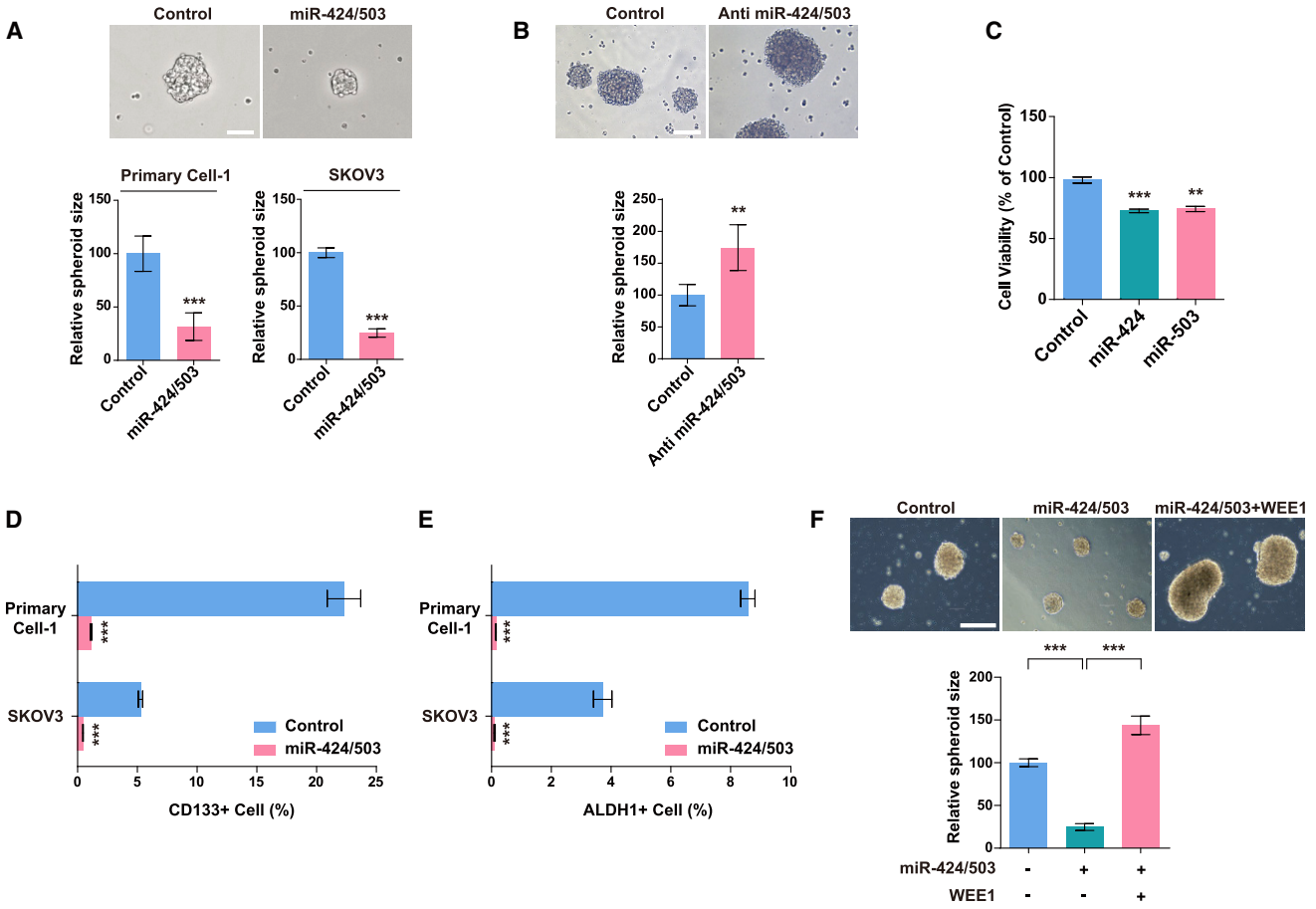

Figure 4. miR-424 and miR-503 inhibit cancer stem cell-like properties in ovarian cancer cells

The sizes of spheroids after the overexpression (A) or inhibition (B) of miR-424/503 in primary ovarian tumor cells and SKOV3 cells. Scale bars: 100 μm. (C) Cell viability after the overexpression of miR-424 and miR-503 in SKOV3 spheroids. (D and E) Fluorescence-activated cell sorting analysis of the CD133- and ALDH1$^+$ subpopulation in primary ovarian cancer cells and SKOV3 cells after miR-424/503 overexpression. (F) Representative images of SKOV3 spheroids, and WEE1 protein expression levels after concurrent miR-424/503 and WEE1 overexpression. Scale bar: 250 μm. $^{**}p < 0.01$, $^{***}p < 0.001$ compared with controls by unpaired two-tailed Student's t test or one-way ANOVA with Bonferroni's multiple comparison test. Error bars, standard error of the mean.

miR-424 and miR-503 decreased more significantly than that from control cells (Figure 5A), which was consistent with the results obtained using the transient overexpression of miR-424 and miR-503 (Figure 4A). Moreover, spheroid formation from control SKOV3 cells was not significantly affected by carboplatin treatment, whereas that from SKOV3 cells expressing miR-424 and miR-503 was reduced substantially on carboplatin treatment (Figure 5A), indicating that miR-424 and miR-503 enhanced the dissociation of the established spheroids in response to this treatment. Interestingly, the reduction in spheroid formation was associated with the induction of apoptosis, because the level of active caspase-3 increased in response to carboplatin treatment (Figure S9). Collectively, these findings support the critical role of the miR-424/503 signaling pathway in determining the cancer stem cell-like characteristics and countering CSC-related chemoresistance in ovarian cancer. The *in vitro* studies demonstrated that the overexpression of miR-424 and miR-503 prevented spheroid formation and, in combination with chemotherapeutics, significantly enhanced spheroid dissociation. To investigate the relevance of these findings *in vivo*, we examined the effects of miR-424 and miR-503 overexpression in an intraperitoneal (i.p.) ovarian cancer model. Ascites development was significantly inhibited in the miR-424/503 overexpression and miR-424/503 overexpression/carboplatin combination groups compared with that in the control group (data not shown). We observed extensive peritoneal metastasis in control mice compared with that in miR-424/503-overexpressing and/or carboplatin-treated mice, because the spread of the tumors to the peritoneal cavities decreased in the latter (Figure 5B). The tumor burden, which is measured by counting the number of tumor nodules, was significantly lower in the miR-424/503 overexpression group than in the control group, and tumor seeding was substantially inhibited in the miR-424/503 overexpression/carboplatin combination group (Figure 5B). Notably, WEE1 expression was persistently increased a week after vehicle or carboplatin treatment in the SKOV3 tumors. Conversely, WEE1 expression was markedly decreased in the

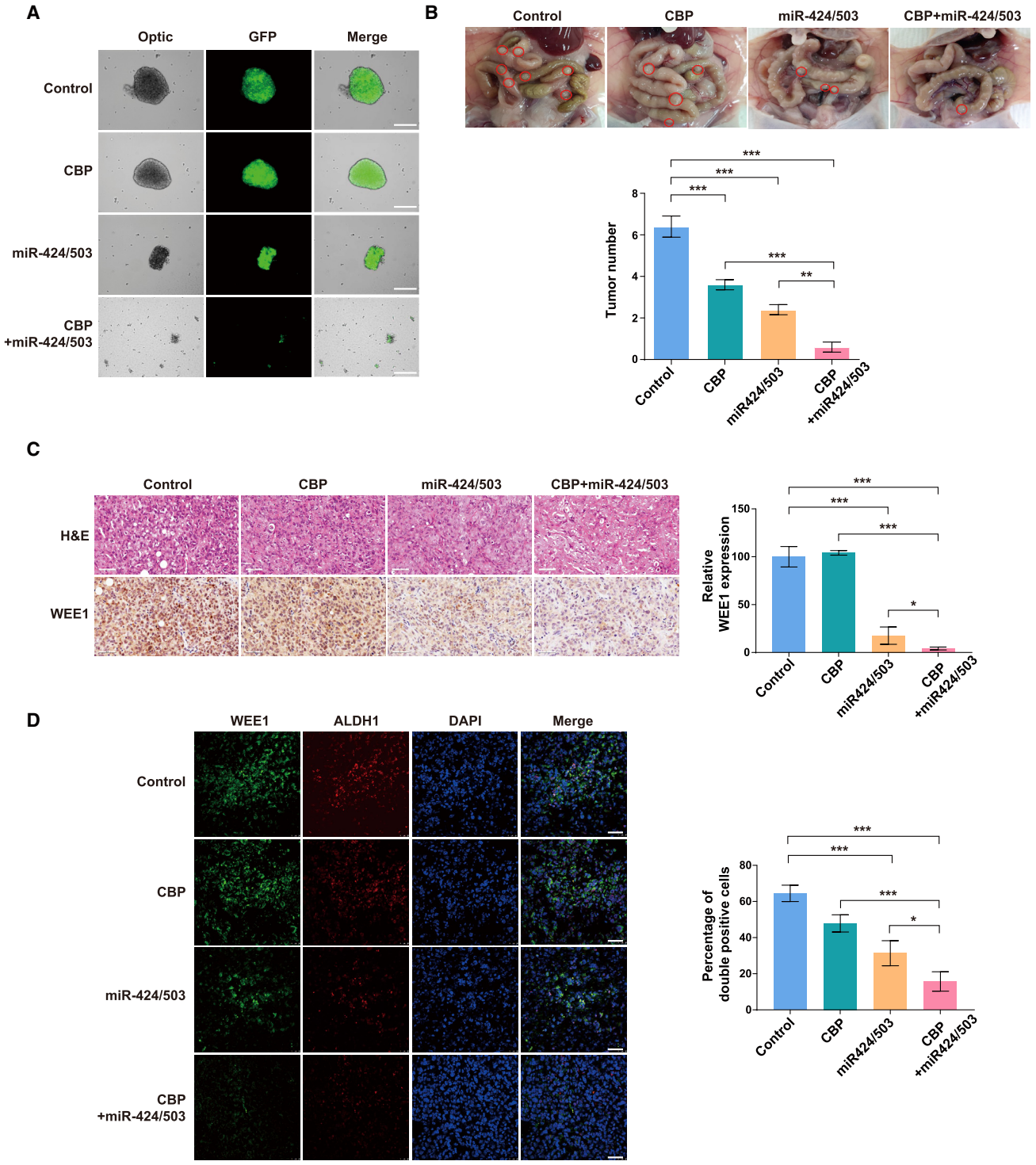

Figure 5. Effect of miR-424/503 expression on the reduction of chemoresistance

(A) Representative images of SKOV3 spheroids in the four different groups. miR-424/503 overexpression enhanced the dissociation of spheroids under carboplatin (CBP) treatment. Scale bar: 250 μm. (B) Representative images of the peritoneal cavities of mice at 4 weeks after implantation. Total tumor number graphs show decreased peritoneal metastasis in the CBP, miR-424/503, and CBP/miR-424/503 groups compared with the control group. The CBP/miR-424/503 significantly lowered the tumor number compared with the CBP or miR-424/503 group. Based on $\alpha = 0.05$, the effect size of the four groups (n = 32) is 2.57, and the power is 0.99 or higher. **p < 0.01,

(legend continued on next page)

miR-424 and miR-503 overexpression group (Figure 5C), which indicated the importance of the miR-424/503-WEE1 axis in peritoneal implantation metastasis and overcoming chemoresistance in ovarian cancer. Finally, to further clarify the relationship between miR-424/503-mediated WEE1 expression and CSC-like phenotype *in vivo*, we carried out double-immunostaining analysis of ALDH1 and WEE1 in the SKOV3 tumors. Morphometric analysis of fluorescence intensities for ALDH1, WEE1, and ALDH1/WEE1 (co-localization) demonstrated that the control tumors showed high expression of WEE1 and ALDH1. WEE1 expression was significantly correlated with ALDH1 expression. Of note, about 65% of $ALDH1^+$ tumor cells showed WEE1 expression as indicated by co-localization in the control group. Fluorescence intensities for ALDH1, WEE1, and ALDH1/WEE1 (co-localization) showed significant decreases in the miR-424/503 overexpression and miR-424/503 overexpression/carboplatin combination group. These results further supported our findings *in vitro*, which had demonstrated that WEE1 expression is closely correlated with CSC properties in ovarian cancer (Figure 5D).

NANOG upregulates WEE1 expression by suppressing miR-424 and miR-503 expression

Next, we attempted to identify an upstream regulator that might be involved in the regulation of the miR-424/503-WEE1 axis. Previous studies have shown that the transcription factor NANOG expression was significantly associated with reduced chemosensitivity and poor OS and disease-free survival. In addition, the inhibition of NANOG expression decreased WEE1 expression in human colorectal cancer, suggesting a significant involvement of NANOG in the miR-424/503-WEE1 axis.[50,51] Hence it was hypothesized that NANOG may contribute to the regulation of cancer stem cell-like characteristics in ovarian cancer cells via modulation of the miR-424/503-WEE1 axis. To confirm the potential involvement of NANOG in the regulation of cancer stem cell-like characteristics via the miR-424/503-WEE1 axis, we measured the NANOG expression level in ovarian cancer spheroids. Both mRNA and protein levels of NANOG were increased in the SKOV3 and OVCAR8 spheroids (Figures 6A–6C). To determine whether NANOG is involved in the regulation of miR-424/503 and WEE1 expression, we examined the effects exerted by NANOG overexpression on miR-424/503 and WEE1 expression in ovarian cancer cells. We found that miR-424 and miR-503 expression were significantly downregulated in response to NANOG overexpression (Figure 6D). We also found that WEE1 expression was significantly upregulated in response to NANOG overexpression in ovarian cancer cells, which indicated the involvement of NANOG in the regulation of miR-424/503-mediated WEE1 expression (Figures 6E and 6F). These findings were verified by analysis of publicly available ovarian cancer datasets from the National Center for Biotechnology Information (GEO: GSE30161); an inverse correlation between NANOG levels and levels of miR-424/503 was confirmed, whereas WEE1 and NANOG had a significant positive correlation (Figure S3A). Finally, to further investigate the relationship between NANOG and the miR-424/503-WEE1 axis, we examined whether the NANOG-mediated WEE1 upregulation is regulated by miR-424/503. We found that the increase in WEE1 expression observed with NANOG overexpression was reduced on the concurrent overexpression of miR-424 and miR-503 (Figures 6G and 6H), which indicated that in ovarian cancer cells, NANOG-regulated WEE1 expression is mediated, at least in part, by miR-424 and miR-503. Finally, we examined the expression of pri-forms of miR-424/miR-503 to evaluate whether NANOG regulates transcription of miR-424 and 503 or post-transcriptional maturation. We found that both the pri (Figure S10A) and mature forms (Figure 6D) of miR-424 and miR-503 were significantly downregulated by NANOG overexpression, suggesting that the transcription of these miRNAs, rather than their post-transcriptional maturation, is regulated by NANOG. We also found the robust reduction of luciferase reporter driven by putative promoter region of miR-424/503 by NANOG overexpression (Figure S10B). Collectively, these findings suggest that NANOG regulates miR-424 and miR-503 expression, which in turn directly regulates the WEE1 expression in ovarian cancer. However, further investigations are required to clarify the precise mechanism by which NANOG regulates miR-424 and miR-503 expression in ovarian cancer.

Atorvastatin regulates cancer stem cell-like characteristics in ovarian cancer cells by modulating the NANOG-miR-424/503-WEE1 axis

To further validate the role of the NANOG-miR-424/503-WEE1 axis in regulating cancer stem cell-like characteristics in ovarian cancer cells, we attempted to design a pharmacological strategy to restore the altered NANOG-miR-424/503-WEE1 axis in ovarian cancer spheroids.

Data from previous studies on endothelial cells showed that the expressions of miR-424 and miR-503 are closely regulated by apelin/APJ signaling. Statins can augment apelin/APJ signaling, which suggests that statins may regulate miR-424/503 expression as well.[44,52] In addition, several studies have demonstrated the therapeutic potential of statins; they can inhibit tumor growth and metastasis in various types of cancer, including melanoma, breast cancer, and ovarian cancers,[53–55] and downregulate pluripotency markers such as NANOG and OCT-4 in embryonic stem cells and breast cancer cells.[56,57] We assessed the effect of atorvastatin on miR-424 and miR-503 expression and found that the expression levels of miR-424 and miR-503 in ovarian cancer spheroids were restored in response to atorvastatin treatment (Figure 7A). To confirm the role of the NANOG-miR-424/503-WEE1 axis, we evaluated whether atorvastatin can inhibit NANOG and WEE1 expression. The upregulation of NANOG and WEE1 expression in ovarian cancer spheroids was reversed on treatment

***$p < 0.001$ by one-way ANOVA with Bonferroni's multiple comparison test. (C) Hematoxylin and eosin staining and immunostaining for WEE1 in tumors from the four different groups. Scale bar: 50 μm. (D) Representative fluorescence profiles for ALDH1, WEE1, and ALDH1/WEE1 colocalization in the CBP, miR-424/503, and CBP/miR-424/503 groups compared with that in the control group. The graphs show significantly decreased fluorescence intensities for ALDH1, WEE1, and ALDH1/WEE1 (co-localization) in the miR-424/503 overexpression and miR-424/503 overexpression/carboplatin combination group compared with that in mice injected with control cells. Scale bar: 50 μm. *$p < 0.05$, ***$p < 0.001$ by one-way ANOVA, with Bonferroni's *post hoc* test.

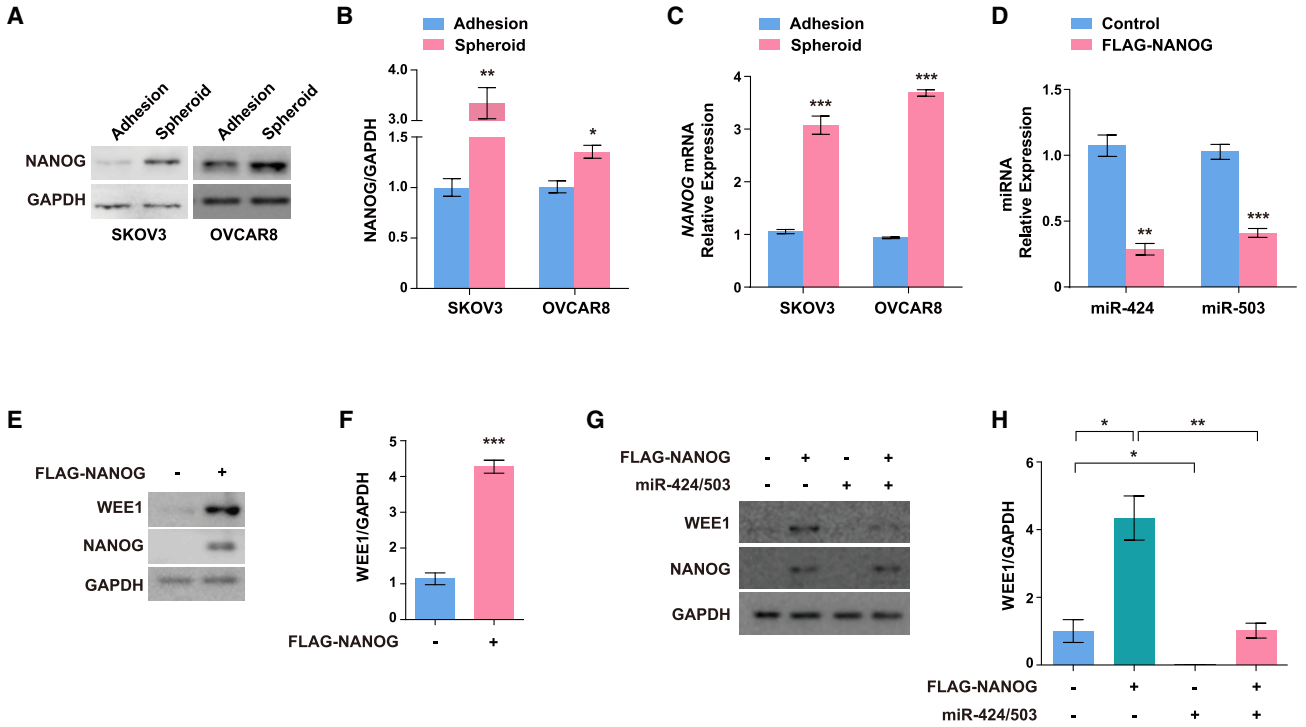

Figure 6. NANOG upregulates WEE1 expression by downregulating miR-424 and miR-503 expression

(A–C) Protein and mRNA levels of NANOG in SKOV3 and OVCAR8 adherent cells and spheroids. (D) Mature miR-424 and miR-503 expression in response to NANOG overexpression. (E and F) WEE1 protein expression in response to NANOG overexpression. (G and H) WEE1 protein expression in response to miR-424/503 overexpression with concurrent NANOG overexpression. *$p < 0.05$, **$p < 0.01$, ***$p < 0.001$ compared with controls by unpaired two-tailed Student's t test or one-way ANOVA with Bonferroni's multiple comparison test. Error bars, standard error of the mean.

with atorvastatin (Figures 7B–7D). Next, we examined whether atorvastatin regulates the cancer stem cell-like properties of ovarian cancer cells. Atorvastatin significantly decreased the viability of spheroid cells and inhibited spheroid formation from primary ovarian tumor cells and SKOV3 cells (Figures 7E and 7F). Moreover, to investigate whether atorvastatin inhibits ovarian cancer stem cell-like properties, we examined the typical characteristics of CSCs, such as their self-renewal potential and expression of representative CSC markers.[58] The self-renewal potential was determined using the *in vitro* limiting dilution assay. The graph showed that atorvastatin treatment induced the serial exclusion of self-renewing cells (Figure 7G), which indicated that the self-renewing activity of ovarian CSCs was inhibited. In addition, atorvastatin significantly decreased the percentage of $ALDH1^+$ cells among primary ovarian cancer cells and SKOV3 cells (Figure 7H). Collectively, the results suggest that atorvastatin attenuates cancer stem cell-like properties in ovarian cancer cells by engaging the NANOG-miR-424/503-WEE1 signaling axis.

Combination of atorvastatin and carboplatin suppressed tumor growth and peritoneal seeding in a mouse model of i.p. ovarian cancer

The *in vivo* studies demonstrated that miR-424 and miR-503 overexpression/carboplatin combination treatment substantially inhibited the tumor seeding (Figure 5B); we also confirmed that the expression levels of miR-424 and miR-503 in ovarian cancer spheroids were restored on atorvastatin treatment (Figure 7A). Furthermore, we demonstrated that atorvastatin suppresses the cancer stem cell-like characteristics in ovarian cancer cells by modulating the NANOG-miR-424/503-WEE1 axis. We evaluated the combinatorial effect of atorvastatin and carboplatin on tumor growth and peritoneal seeding in an i.p. mouse model of SKOV3 cells. First, to confirm the safety of atorvastatin, carboplatin, and their combined treatment, we measured the body weight of each mouse. During the drug treatment, no significant changes were observed in body weights among the different groups, indicating that the combination of atorvastatin and carboplatin exerted no obvious side effects (Figure S11). Next, we examined ascites development in mice inoculated i.p. Ascites development was significantly inhibited in the group treated with carboplatin compared with that in the control group and was also substantially inhibited in the atorvastatin/carboplatin combination group (Figures 8A and 8B). In addition, the atorvastatin/carboplatin combination substantially reduced peritoneal seeding compared with that in the control group in the mouse model of i.p. SKOV3 ovarian cancers (Figure 8C). To better convey broad applicability, we replicated the experiment in an i.p. mouse model of OVCAR3, OVCAR5, and OVCAR8 cells, obtaining a similar result (Figures 8C and S12).

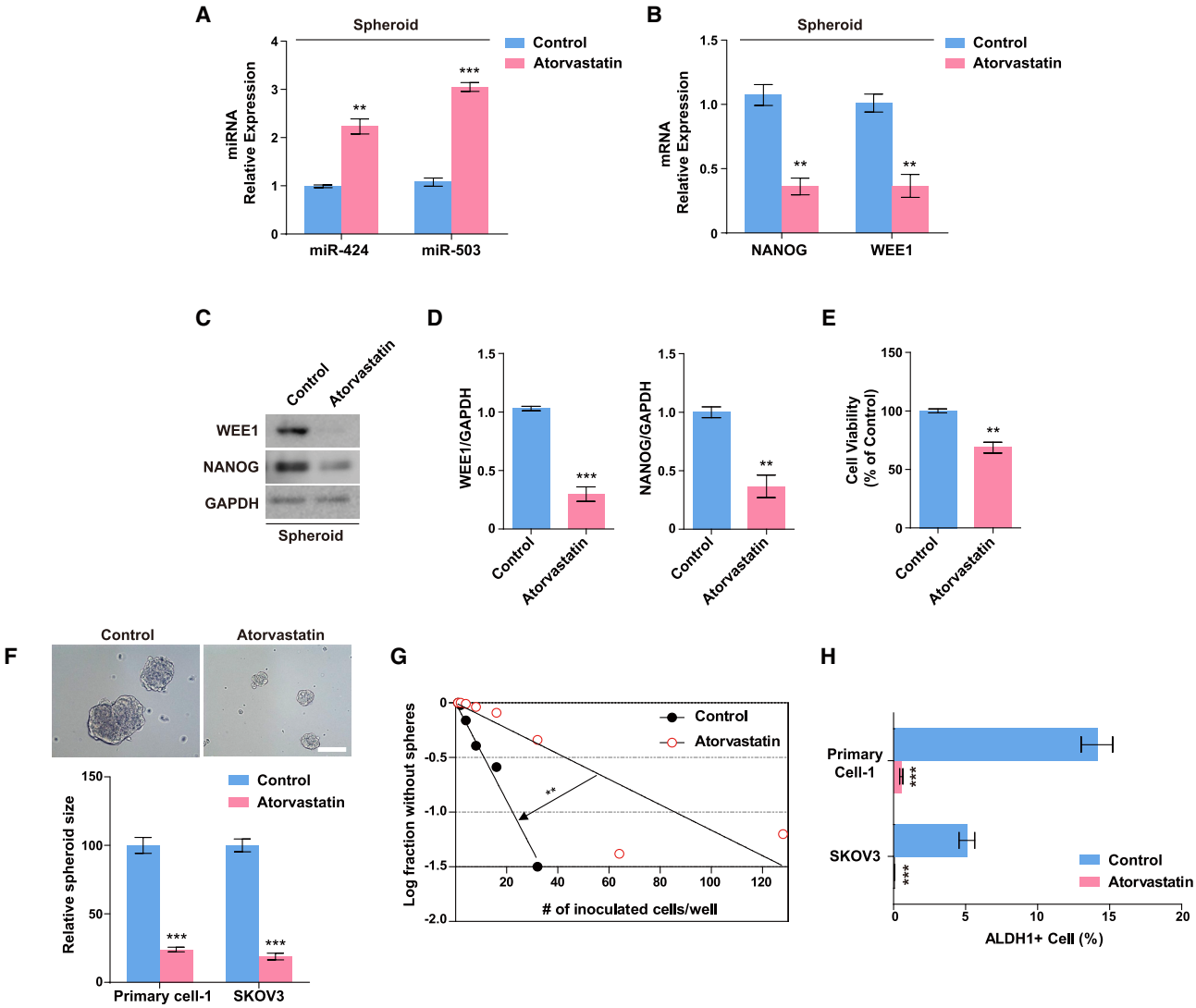

Figure 7. Atorvastatin regulates ovarian cancer stem cell-like properties by modulating the NANOG-miR-424/503-WEE1 axis in SKOV3 spheroids

(A) Mature miR-424 and miR-503 expression in SKOV3 spheroids in response to treatment with 10 μM atorvastatin. NANOG and WEE1 mRNA (B) and protein (C and D) expression in SKOV3 spheroids in response to treatment with 10 μM atorvastatin. (E) Viability of SKOV3 spheroids after treatment with 10 μM atorvastatin for 24 h. (F) Representative images of SKOV3 spheroids after treatment with 10 μM atorvastatin. The sizes of the spheroids formed from SKOV3 cells treated with 10 μM atorvastatin were significantly smaller compared with the control. $^{**}p < 0.01$, $^{***}p < 0.001$ compared with controls by unpaired two-tailed Student's t test (A–E). Error bars, standard error of the mean. (G) Limiting dilution assay showing the decreased self-renewal activity of SKOV3 spheroids in response to treatment with 10 μM atorvastatin. $^{**}p < 0.01$ for groups (control, atorvastatin), cells/well, and groups × cells/well by two-way ANOVA with Bonferroni's multiple comparison test. (H) Fluorescence-activated cell sorting analysis of ALDH1$^+$ SKOV3 spheroids after treatment with 10 μM atorvastatin. Scale bar: 100 μm. $^{***}p < 0.001$ compared with controls by unpaired two-tailed Student's t test. Error bars, standard error of the mean.

Carboplatin significantly inhibited tumor growth even when administered alone, and the combination of atorvastatin and carboplatin further inhibited tumor growth (Figures 8D and 8E). Furthermore, we demonstrated that miR-424/503 expression in the tumors increased in the atorvastatin and atorvastatin/carboplatin combination groups, but in comparison with the results of the control group, miR-424/503 expression showed no significant change in the carboplatin group (Figure 8F). We also found that WEE1 and NANOG expression in the tumors decreased in the atorvastatin and atorvastatin/carboplatin combination groups but remained unaffected in the carboplatin group (Figures 8G and 8H).

These results suggest that in the peritoneal metastasis model of ovarian cancer developed using spheroids, tumor metastasis was suppressed, and sensitivity to carboplatin was improved after treatment with atorvastatin because of the inhibition of the typical cancer

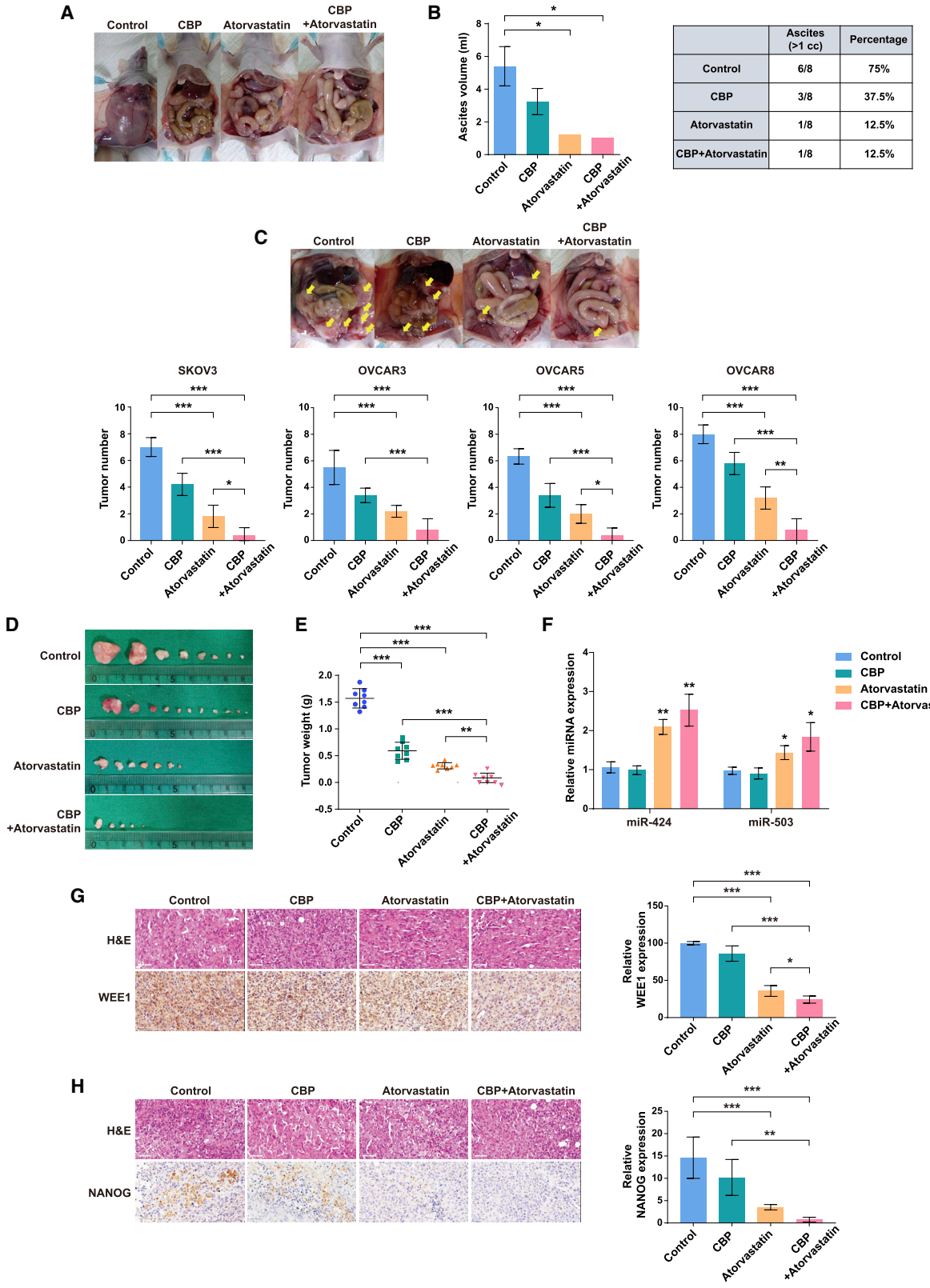

	Ascites (>1 cc)	Percentage
Control	6/8	75%
CBP	3/8	37.5%
Atorvastatin	1/8	12.5%
CBP+Atorvastatin	1/8	12.5%

(legend on next page)

stem cell-like properties through the regulation of the NANOG-miR-424/503-WEE1 signaling axis.

DISCUSSION

Clinically recurrent ovarian cancer, which is mostly incurable, is categorized on the basis of platinum-free interval (PFI), which is the most important predictive factor for the response to subsequent lines of chemotherapy. Patients with a PFI of more than 6 months after the initial platinum-based therapy are considered platinum sensitive, whereas patients with a PFI of less than 6 months are considered platinum resistant.[59] While treating a platinum-sensitive recurrent disease, poly (adenosine diphosphate [ADP]–ribose) polymerase (PARP) inhibitors are considered standard-of-care maintenance therapy for patients who have not been previously treated with this kind of drug.[60–63] However, platinum-resistant recurrent ovarian cancer has a poor prognosis. More effective treatment of platinum resistance or, preferably, its prevention or reversal remains a priority. Accumulating evidence indicates that CSCs are emerging as critical mediators of drug resistance in ovarian cancer.[5,64] Furthermore, numerous studies have reported that the expression level of WEE1 increased in different cancer types, such as breast cancer,[13,65] ovarian cancer,[16,66] colorectal cancer,[67] gastric cancer,[68] malignant melanoma,[15] and sarcoma.[69] In ovarian cancer, WEE1 expression is significantly higher after exposure to chemotherapy, and high WEE1 expression was significantly correlated with poor survival outcomes, suggesting the role of WEE1 as a novel prognostic marker and therapeutic target in ovarian cancer.[16] WEE1 expression imparts cells with the ability to survive under stressful conditions and maintain a stem-like state.[14,70,71] In this respect, the role of WEE1 in CSCs and drug resistance in ovarian cancer were investigated in this study. Here, we showed that WEE1 plays a key role in regulating the action of CSCs and tumor resistance to carboplatin via a miRNA-dependent mechanism in ovarian cancer. The findings suggested that the resistance of CSC populations to DNA-damaging treatments can be overcome by WEE1 inhibition. Moreover, miR-424/503-mediated WEE1 inhibition re-sensitized chemoresistant ovarian cancer cells to carboplatin. In the i.p. ovarian cancer xenograft model, miR-424/503 overexpression significantly reduced the peritoneal metastasis of tumors and improved survival compared with that achieved using carboplatin treatment alone. These results indicated that the functional modulation of the miR-424/503-WEE1 axis may help suppress platinum resistance in CSCs for improving outcomes after a platinum-resistant relapse, which constitutes a major obstacle in the clinical management of ovarian cancer.

Adavosertib (AZD1775), a highly selective WEE1 inhibitor, was developed with the aim of sensitizing tumor cells lacking functional p53 expression to various DNA-damaging agents and radiotherapy by abrogating the G2 DNA damage checkpoint.[72,73] Preclinical studies on adavosertib demonstrated the induction of cell death and sensitization of tumor cells to gemcitabine, carboplatin, and cisplatin treatment in ovarian cancer.[74–76] The increase in activity was also shown to depend on the p53 status, with greater selectivity toward p53-defective cells. High-grade serous carcinomas (HGSCs), the cause of 70% of ovarian carcinoma-related deaths, are characterized by *TP53* gene mutations, which are detected in more than 95% of the cases.[77] The WEE1 inhibitor adavosertib might be a potential therapeutic agent against HGSC. Recent clinical trials for adavosertib in combination with DNA-damaging agents have shown encouraging results against relapsed ovarian cancer. In a randomized phase II study of platinum-sensitive recurrent disease (ClinicalTrials.gov: NCT01357161), combining adavosertib with paclitaxel and carboplatin improved response (objective response rate [ORR], 74.6%) and PFS (median, 7.9 months; HR, 0.63; $p = 0.080$).[78] In a double-blind, randomized phase II study of platinum-resistant disease (ClinicalTrials.gov: NCT02151292), combined treatment with adavosertib and single-agent gemcitabine improved response (ORR, 23.0%, $p = 0.038$), PFS (median, 4.6 months; HR 0.55; $p = 0.015$), and OS (median, 11.4 months; HR 0.56; $p = 0.017$).[79] Notably, this was the first randomized trial to report a significant improvement in OS and PFS in a platinum-refractory and platinum-resistant disease. The improvement of OS is important in ovarian cancer trials; however, it remains challenging to achieve this clinically. Among the targeted therapies used for recurrent ovarian cancers in clinical settings, only bevacizumab (an anti-vascular endothelial growth factor antibody [Ab]) combined with standard platinum-based chemotherapy significantly improved the median OS in patients with platinum-sensitive recurrent ovarian cancer;[80] no significant improvements were observed in patients with platinum-resistant recurrent ovarian cancer.[81] Meanwhile, published phase II studies of recurrent ovarian cancer therapy combining adavosertib and DNA-damaging agents reported significant improvements in the median OS of patients with platinum-resistant recurrent disease, but not platinum-sensitive recurrent disease. The mitotic lethality rationale of adavosertib, based

Figure 8. Combined treatment with carboplatin and atorvastatin inhibited ovarian cancer in the ovarian cancer xenograft mouse model

(A) Representative images of ascites development at 4 weeks after tumor implantation. (B) Graphs showing significantly decreased ascites development in the atorvastatin or atorvastatin/carboplatin (CBP) treatment groups compared with that in the CBP treatment group (n = 8) (measurement >1 cc). *$p < 0.05$ compared with controls by one-way ANOVA with Bonferroni's multiple comparison test. Error bars, standard error of the mean. The standard deviation is zero because the number of cases is one in atorvastatin and atorvastatin/CBP groups. (C) Representative images of the peritoneal cavities of mice showing a reduction in peritoneal tumors in the CBP, atorvastatin, and atorvastatin/CBP groups compared with that in the control group and quantification of peritoneal metastases. (D and E) Comparative images and tumor weight analysis showed that the atorvastatin/CBP group had higher metastasis-suppressive ability than the CBP and atorvastatin groups. Based on $\alpha = 0.05$, the effect size of the four groups (n = 32) is 4.35, and the power is 0.99 or higher. The sum of all visible tumor weights in each mouse was used as its tumor weight, and each point represents tumor volumes from eight mice. **$p < 0.01$, ***$p < 0.001$ by one-way ANOVA with Bonferroni's multiple comparison test. (F) Mature miR-424 and miR-503 expression in xenograft tumors for four groups. *$p < 0.05$, **$p < 0.01$ compared with controls by unpaired two-tailed Student's t test. (G and H) Hematoxylin and eosin staining and immunostaining for WEE1 and NANOG in xenograft tumors for four groups. Scale bars: 50 μm. *$p < 0.05$, **$p < 0.01$, ***$p < 0.001$ by one-way ANOVA with Bonferroni's multiple comparison test.

on overriding the G2 checkpoint, is that adavosertib will sensitize p53-defective tumor cells to DNA-damaging agents without affecting normal cells with wild-type p53. In fact, the p53-dependent antitumor effects of adavosertib have been identified in several cancer types.[72–74,82] Consistently, in platinum-sensitive ovarian cancer, the clinical benefit (ORR and PFS) of adavosertib has also been reported in patients with different *TP53* mutation subtypes.[78] However, in platinum-resistant ovarian cancer, adavosertib treatment did not yield different results based on the p53 status, despite the superior clinical benefit, including significant OS improvement.[79] Because adavosertib showed significant association with OS improvement in platinum-resistant relapsed disease with CSC enrichment, and no association between the p53 status and clinical benefit was reported, adavosertib may be expected to suppress CSCs involved in platinum resistance beyond its role in the mechanism underlying cell-cycle checkpoint deregulation.

It is well known that miRNAs play a role in cell-cycle differentiation, self-renewal, invasion, and the survival ability of CSCs. For example, miR-34a induces cell-cycle arrest and apoptosis and inhibits tumor growth by negatively regulating various cell-cycle regulators and CSC markers in glioblastomas and $CD44^+$ prostate cancer cells.[83,84] Members of the miR-15a/15b/16/195/424/497/503 family share the same seed sequence and have been shown to cooperatively regulate multiple cell-cycle genes leading to regulation of cell proliferation.[85,86] Specifically, miR-16 and miR-424 inhibit CCNE1, CCND3, and CDK6 to induce cell-cycle arrest and have strong inhibitory effects on cell growth.[85] In addition, the miRNAs of the miR-15/16/195/424/497 family sensitize cisplatin-resistant cells to apoptotic cell death by directly targeting cell-cycle kinases, including WEE1 and CHK1.[87] Nevertheless, the regulatory roles of the members of the miR-15 family in ovarian CSCs remain unclear. A previous study showed that miR-424 was downregulated only in ovarian cancer spheroids.[43] In our prior study, we showed that miR-424 and miR-503 are derived from the same primary transcript and perform similar functions because of substantial identity in their seed sequences.[44,45] In addition, several studies have revealed the roles of miR-424 and miR-503 as tumor suppressors and highlighted their inhibitory effect on cancer cell proliferation, angiogenesis, and chemoresistance in several gynecological cancers.[48,88,89] The expression of these miRNAs is downregulated in ovarian cancer and correlates with the OS of patients[46,90]; however, the mechanism underlying anti-neoplastic regulation by miR-424 and miR-503 in recurrent ovarian cancer remains unclear. In this study, we focused on these miRNAs to elucidate the regulatory roles in ovarian CSCs. We found that the upregulation of WEE1 in ovarian cancer spheroids is associated with decreased miR-424 and miR-503 expression. The overexpression of miR-424 and miR-503 inhibits tumorigenic functions, including colony formation and cell proliferation, and reduces chemoresistance to carboplatin in ovarian cancer cells. In an i.p. ovarian cancer model, miR-424/503 overexpression significantly reduced the peritoneal metastasis of the tumor and improved survival compared with that achieved with only carboplatin treatment. Our findings further emphasize the important role of miR-424 and miR-503 in ovarian CSCs and demonstrate that miR-424 and miR-503 suppress cancer stem cell-like properties by directly targeting WEE1 in ovarian cancer, overcoming chemoresistance, and suppressing peritoneal implantation metastasis. However, further research is needed to fully determine the potential roles of miR-15, miR-16, miR-195, and miR-497 in the context of ovarian CSCs because the members of the miR-15/16/195/424/497 family share several common targets including WEE1.

Disruption of miRNA expression is associated with the pathogenesis of multiple diseases[91]; thus, restoration of the abnormal expression of miRNAs may serve as a promising option in the treatment of various diseases. Here, we showed that the intratumoral injection of lentivirus-expressing miR-424/503 into established ovarian tumors effectively induced tumor regression. Overall, our current study provides the foundation for a potentially novel therapeutic strategy to pursue miRNAs as therapeutic agents for ovarian cancer, a disease that still faces an exceedingly high mortality rate. Although miRNA-based therapeutics provide an attractive anticancer approach, the main limitation in the clinical application is the specific delivery of miRNAs to cancer cells. Therefore, it is critically important to develop targeted therapeutic agent delivery systems such as engineered nanoparticles. Small-molecule-based therapy that can restore the expression of miRNAs to the normal level through modulation of transcription factor or signaling pathways can also be an alternative strategy.

NANOG is a transcription factor involved in the development and reprogramming of adult embryonic stem cells.[92] In addition, NANOG induces the malignant transformation of normal cells into cancer cells.[93] High NANOG expression was shown to be associated with epithelial-to-mesenchymal transition (EMT), chemoresistance, and poor prognosis in ovarian cancer.[66,94] Furthermore, NANOG is closely associated with the properties of CSCs, and spheroid-forming ovarian cancer cells exhibit high NANOG expression.[64,95,96] Mechanistic investigations of the role of NANOG on the stemness of human colorectal cancer cells revealed that NANOG inhibition decreased WEE1 expression, suggesting the potentially crucial involvement of NANOG in the miR-424/503-WEE1 axis.[51] In the present study, we further demonstrated that the expression of NANOG, which is elevated in ovarian cancer spheroids, reduced the expression of miR-424 and miR-503, thereby leading to an increase in WEE1 expression. Transcription factors linked to CSCs, such as NANOG, OCT4, and SOX2, act as transcriptional activators or repressors, and the activities of these transcription factors are ultimately controlled by co-activators and co-repressors. Although a number of prior studies have focused on the role of NANOG as a transcriptional activator in various contexts, several studies have shown that NANOG can also act as a transcriptional repressor by interacting with multiple transcription factors, including OCT4, SOX2, GLI-1, nuclear factor κB (NF-κB), and STAT3, and associating with multiple repressor proteins, such as NCOR1/2, NuRD, and Sin3.[97–99] In addition, NANOG and the repressor proteins co-occupy NANOG-target genes to control gene transcription and cell fate. Therefore, elucidation is required of the unique repressor proteins interacting with

NANOG to regulate the expression of miR-424/503 in the context of ovarian CSCs. In addition, given that NANOG, OCT4, and SOX2 together communicate with distinct repression complexes to control gene transcription, we also need to characterize the mechanism underlying the regulation of miR-424/503 expression and functions in ovarian CSCs via NANOG, OCT4, and SOX2 interaction. Although our current study focused on the novel role of WEE1 as part of a "tuning" mechanism for the regulation of ovarian CSC-like properties, linking the decreased expression of miR-424 and -503 to WEE1 upregulation in ovarian cancer spheroids, and the role of NANOG in the transcriptional regulation of miR-424/503 expression has been partly demonstrated, we need to conduct further experiments to fully elucidate the regulatory mechanism of the miR-424/503-WEE1 axis mediated by NANOG in the context of ovarian CSCs.

Statins, known to inhibit cholesterol synthesis, exhibit anticancer effects, such as cell death induction and EMT inhibition, because cholesterol is a structural component of the cell membrane and is necessary for cellular proliferation and migration.[100] In addition, the inhibition of the mevalonate pathway by statins is associated with the reduced risk of cancer recurrence.[101,102] However, the effect of statins on ovarian CSCs is not well understood yet. Here, the role of statins as anticancer agents and their effects on the miR-424/503-WEE1 axis were evaluated. Atorvastatin induces cytotoxicity in SKOV3 cells and modulates the miR-424/503-WEE1 axis by suppressing NANOG expression, which leads to the inhibition of spheroid formation. Statins have been shown to suppress the expression of cancer stemness markers only in cells with abnormal genome integrity.[57]

In this study, the levels of known CSC markers expressed in ovarian CSCs, spheroid formation, spheroid cell viability, and the self-renewing activity of ovarian CSCs were decreased by atorvastatin, suggesting this drug attenuates cancer stem-like properties by regulating the miR-424/503-WEE1 axis in ovarian cancer cells. Given that CSCs are resistant to chemotherapeutic agents and cause cancer relapse, the development of drugs that selectively target CSCs offers great promise for cancer treatment, especially in combination with chemotherapeutic agents. Here, we demonstrated that combined treatment with atorvastatin and carboplatin suppressed tumor growth and peritoneal seeding in a mouse model of i.p. ovarian cancer. These findings indicate that atorvastatin, when administered in combination with standard chemotherapeutic drugs, may be a promising therapy for ovarian cancer owing to its ability to inhibit cancer stem cell-like properties in the ovarian cancer cell population by modulating the NANOG-miR-424/503-WEE1 axis. These findings also support the potential application of atorvastatin in preventing ovarian cancer recurrence and as an adjuvant therapeutic in combination with standard chemotherapeutics; however, more *in vivo* animal studies and clinical trials are needed in this area of research.

Conclusions

In summary, given that CSCs mediate tumor resistance to chemotherapy and may contribute to cancer relapse, there is an urgent need to develop therapeutic strategies that target CSCs. Our findings provide evidence that the NANOG-miR-424/503-WEE1 signaling axis plays a pivotal role in the regulation of ovarian CSCs, and this axis can be regulated by atorvastatin. We propose that WEE1 inhibition in combination with conventional DNA-damaging chemotherapy may have potential applications in the prevention of ovarian cancer relapse.

MATERIALS AND METHODS

Cell culture and transfection

Human ovarian cancer cell lines (SKOV3, OVCAR3, OVCAR5, and OVCAR8) were cultured in RPMI-1640 medium (HyClone, Logan, UT, USA) supplemented with 10% fetal bovine serum (FBS; HyClone), 1% penicillin-streptomycin (WelGENE, Deagu, Korea), and mycozap (Lonza, Walkersville, MD, USA) at 37°C in a 5% CO_2 incubator. Lipofectamine RNAiMAX (Invitrogen, Carlsbad, CA, USA) was used for *in vitro* miRNA and small interfering RNA (siRNA) transfection according to the manufacturer's instructions. Ambion (Austin, TX, USA) miR-424 precursor (PM10306), miR-503 precursor (PM10378), miR-424 inhibitor (catalog no. [Cat.] 4464084), and miR-503 inhibitor (Cat. 4464084) were used as previously described.[44,45] Validated *WEE1* siRNAs (Cat. 7465-1 and 7465-2) and negative control siRNA (Cat. SN-1003) were purchased from Bioneer (Daejeon, Korea). Two independent siRNA sequences were used to silence WEE1 expression: the *WEE1* siRNA sequence 1 was sense 5′-CUUUUACUCCGGAUUCUUU(dTdT)-3′ and antisense 5′-AAAGAAUCCGGAGUAAAAG(dTdT)-3′, and the *WEE1* siRNA sequence 2 was sense 5′- GAGAACGUAUUGGAAUGAU(dTdT)-3′ and antisense 5′- AUCAUUCCAAUACGUUCUC(dTdT)-3'. Plasm id DNA constructs were transfected into the cells using polyethylenimine (Polysciences, Warrington, PA, USA) according to the manufacturer's instructions. Dr. Kyung-Hee Chun (Yonsei University, Korea) and Dr. Sung Hee Baek (Seoul National University, Korea) kindly provided us with the pcDNA-3X Flag-WEE1 plasmid DNA and pcDNA-Flag-NANOG, respectively.

Preparation of human tissue specimens

The study protocol was reviewed and approved by the Institutional Review Board of Pusan National University Hospital (IRB-2001-010-087). All patients enrolled in this study provided informed consent via a signed form before the study commenced. Ovarian cancer tissue was collected during surgery, and its identity was confirmed by a pathologist from the Department of Gynecologic Pathology before it was transferred to the cell culture laboratory. Pathologically confirmed fresh samples were processed using enzymatic and mechanical disassociation into single-cell suspensions and cultured under conditions used for stem cell culture, as described previously.[103,104] RNA and protein were extracted from the tumor tissues.

Animal experiments

Female 7-week-old Balb/C nude mice (Orient Bio., Gyeonggi, Korea) were maintained under a 12-h light/dark cycle, and the experiments were conducted in accordance with the regulations of the Pusan National University Hospital. All procedures were performed in accordance with the policies of the Institutional Animal Care and Use

Committee of Pusan National University of Korea (PNUH-2017-110). For the development of the SKOV3 spheroid tumor model, 1×10^7 dissociated SKOV3 spheroids or SKOV3 spheroid cells overexpressing miR-424/503 were injected i.p. into each mouse. Tumor-bearing mice were randomly divided into four groups (n = 8/group) after 3 days of SKOV3 spheroid injection. Seven days after cell injection, the single-treatment groups were administered carboplatin (50 mg/kg body weight; Cat. C2538; Sigma-Aldrich, St. Louis, MO, USA) weekly or atorvastatin (10 mg/kg body weight; Cat. 10493; Cayman, Ann Arbor, MI, USA) by i.p. injection daily. To avoid toxicity in the case of carboplatin and atorvastatin combination therapy, carboplatin (40 mg/kg body weight) was administered weekly, and atorvastatin (10 mg/kg body weight) was administered i.p. three times a week. The body weight of the mice was measured every 2–3 days from the day of injection. To evaluate the formation of ovarian tumors, we monitored the mice weekly for ascites development and palpable tumor growth. The mice were sacrificed by cervical dislocation on the 28th day after injection, and the abdominal cavity of each mouse was incised to image ascites and the tumors formed in the abdominal cavity. The size of the tumor was measured by separating the tumor formed in the abdominal cavity, and the weight of the separated tumor was measured using a microscale. The tumors were sampled and conditioned for histological analysis (10% formalin fixation).

Immunohistochemistry (IHC)

IHC staining was performed on formalin-fixed, paraffin-embedded tissues using an anti-WEE1 mouse monoclonal Ab (SC-5285; Santa Cruz Biotechnology, Dallas, TX, USA). The ImmPRESS HRP REAGENT kit (MP-7402; Vector Laboratories, Burlingame, CA, USA) was used for IHC staining. Counterstaining was performed using hematoxylin. Images were recorded at a magnification of 400× using the Aperio ImageScope software (Leica Biosystems, Wetzlar, Germany).

Immunofluorescence analyses

Immunofluorescence analyses were performed on the xenograft tumors after they were removed from BALB/c nude mice. The tumors were fixed in 4% paraformaldehyde, paraffin embedded, and cut into 4-μm serial sections. Samples were deparaffinized with xylene, rehydrated using a reduced ethanol gradient, and washed with deionized water. Antigen retrieval was performed in 10 mM citrate buffer using a pressure cooker. After washing with buffer (0.15 M NaCl, 50 mM Tris, and 0.05% Tween 20), endogenous peroxidases were quenched, and the sections were washed with PBS three times. The sections were blocked with 2% goat serum in PBS at 37°C for 45 min and incubated with monoclonal anti-WEE1 (sc-5285 AF488, dilution 1:100; Santa Cruz Biotechnology, Dallas, TX, USA), monoclonal anti-ALDH1 (sc-166362 AF594; dilution 1:100; Santa Cruz Biotechnology, Dallas, TX, USA), and DAPI (62,248, dilution 1:1,000; Thermo Fisher Scientific, Waltham, MA, USA) overnight at 4°C. Images were recorded at a magnification of 400× using the Confocal microscope (Leica Biosystems, Wetzlar, Germany).

Intratumoral injection

To assess whether the lentivirus-expressing miR-424/503 could efficiently induce tumor regression, we injected spheroid SKOV3 cells (5×10^6 cells) in 100 μL saline into both flanks of 6-week-old female BALB/c nude mice divided into four groups (n = 5 per group). Three days after injection, mice of four groups received intratumoral injection of 50 μL of saline, 1×10^8 of virus scramble or virus miR-424/503, and i.p. injection of carboplatin (50 mg/kg) in 100 μL of PBS. The size of the tumor was measured every 3 days using vernier calipers, and after 14 days, mice were sacrificed and the excised tumors were analyzed.

RNA extraction and quantitative real-time PCR

Total RNA was isolated using the miRNeasy RNA isolation kit (QIAGEN, Hilden, Germany), and purified RNA was reverse transcribed using the TaqMan miRNA Reverse Transcription kit (Applied Biosystems, Foster City, CA, USA). miRNA quantitative real-time PCR was performed using the TaqMan Universal Master Mix II (Applied Biosystems). miR-424 and miR-503 were detected using the TaqMan probes. RNAU6B was used as the internal control for the normalization of miR-424 and miR-503. mRNA was reverse transcribed using the qPCRBIO cDNA Synthesis Kit (PCR Biosystems, London, UK). Quantitative real-time PCR was performed using the qPCRBIO SyGreen Mix Hi-ROX (PCR Biosystems) according to the manufacturer's instructions. 18S rRNA was used as the internal control. The sequences of the PCR primers used were as follows: WEE1: forward, 5′-GATGTGCG ACAGACTCCTCAAG-3′, and reverse, 5′-CTGGCTTCCATGTCT TCACCAC-3′; NANOG: forward, 5′-AGTCCCAAAGGCAAACAAC CCACT-3′, and reverse, 5′-TGCTGGAGGCTGAGGTATTTCTGT-3′; Pri-miR-424/503: forward, 5′-ATGTGCGTTTCTAGCTGCTT-3′, and reverse, 5′-TTGAAGTCACGAAGGGCTCC-3′; and 18S rRNA: forward, 5′-ACCCGTTGAACCCCATTCGTGA-3′, and reverse, 5′-GCCTCACTAAACCATCCAATCGG-3′.

Western blotting

The cells were lysed using radioimmunoprecipitation assay (RIPA) buffer (Biosesang, Seongnam, Korea) containing protease inhibitor cocktails (GenDEPOT, Katy, TX, USA). The lysates were centrifuged at 13,000 rpm for 15 min at 4°C for sample preparation. Protein concentrations were measured using a Pierce BCA Protein Assay kit (Thermo Fisher Scientific, Waltham, MA, USA), and equal quantities of protein were boiled and separated using SDS-polyacrylamide gel electrophoresis and transferred onto a polyvinyl difluoride membrane (Millipore, Burlington, MA, USA). The protein bands were hybridized with primary Abs against WEE1 (1:1,000; Cell Signaling, Danvers, MA, USA), NANOG (1:1,000; Cell Signaling), and GAPDH (1:4,000; Cell Signaling). Immunodetection was accomplished using horseradish peroxidase (HRP)-conjugated secondary Abs, and the blots were developed using an enhanced chemiluminescence detection system (Thermo Scientific).

Spheroid formation assay

SKOV3 cells were seeded at 1×10^5 cells/mL in six-well plates coated with poly 2-hydroxylethyl methacrylate (poly-HEMA; Sigma-Aldrich) and cultured in serum-free DMEM/F12 medium (Welgene) supplemented with 20 ng/mL epidermal growth factor (Invitrogen), 10 ng/mL basic fibroblast growth factor (Invitrogen), 0.4% bovine

serum albumin (GenDEPOT), and 5 mg/mL insulin (Sigma-Aldrich). Adavosertib (HY-10993; MedChemExpress, NJ, USA) was added at 200 nM. Spheroid formation was assessed 5 days after seeding. The cells were observed under a microscope at 100× magnification. The sizes of the spheroids were measured using ImageJ software.

Statistical analysis

All experiments were repeated at least three times, and the data shown are the means ± SEM. When only two groups were compared, statistical significance was assessed using an unpaired two-tailed Student's t test. Otherwise, statistical significance was determined using one-way analysis of variance (ANOVA) followed by Bonferroni's multiple comparison test. Relationships between variables were determined by the Pearson correlation coefficient. A p value <0.05 was considered statistically significant (*$p < 0.05$, **$p < 0.01$, ***$p < 0.001$). All statistical analyses were performed using GraphPad Prism v.7.0.

Additional methods

Additional methods are provided in supplemental materials and methods.

Data availability statement

All data are available from the authors on reasonable request.

SUPPLEMENTAL INFORMATION

Supplemental information can be found online at https://doi.org/10.1016/j.omtn.2022.08.028.

ACKNOWLEDGMENTS

We thank Dr. Kyung-Hee Chun (Yonsei University, Korea) and Dr. Sung Hee Baek (Seoul National University, Korea) for kindly providing us with the pcDNA-3X Flag-WEE1 plasmid DNA and pcDNA-Flag-NANOG, respectively. This research was supported by the Basic Science Research Program through the National Research Foundation of Korea (NRF) supported by the Ministry of Education(NRF-2016R1A5A1011974 to J.K. and B.S.K.; NRF-2022R1A2C1003866 to J.K.).

AUTHOR CONTRIBUTIONS

J.K. and B.S.K. designed and supervised the study. J.G.C., S.-W.K., A.L., H.-N.J., E.Y., J.C., S.-W.K., K.H.K., D.S.S., and K.U.C. carried out experiments and analyzed the data. K.H.Y., S.O., and J.C. analyzed computational data. S.J.J. performed the statistical analysis. J.K., B.S.K., J.G.C., S.-W.K., A.L., and H.-N.J. wrote the manuscript. A.L. and S.-W.K. prepared the figures. W.C., J.B.L., S.Y., M.-S.L., J.H.P., M.H.J., S.-W.K., K.H.K., D.S.S., and K.U.C. contributed to the discussion. All authors have read and approved the article.

DECLARATION OF INTERESTS

The authors declare no competing interests.

REFERENCES

1. Sankaranarayanan, R., and Ferlay, J. (2006). Worldwide burden of gynaecological cancer: the size of the problem. Best Pract. Res. Clin. Obstet. Gynaecol. *20*, 207–225.
2. Ferlay, J., Shin, H.R., Bray, F., Forman, D., Mathers, C., and Parkin, D.M. (2010). Estimates of worldwide burden of cancer in 2008: GLOBOCAN 2008. Int. J. Cancer *127*, 2893–2917.
3. Jung, E., Koh, D., Lim, Y., Shin, S.Y., and Lee, Y.H. (2020). Overcoming multidrug resistance by activating unfolded protein response of the endoplasmic reticulum in cisplatin-resistant A2780/CisR ovarian cancer cells. BMB Rep. *53*, 88–93.
4. Steg, A.D., Bevis, K.S., Katre, A.A., Ziebarth, A., Dobbin, Z.C., Alvarez, R.D., Zhang, K., Conner, M., and Landen, C.N. (2012). Stem cell pathways contribute to clinical chemoresistance in ovarian cancer. Clin. Cancer Res. *18*, 869–881.
5. Bapat, S.A., Mali, A.M., Koppikar, C.B., and Kurrey, N.K. (2005). Stem and progenitor-like cells contribute to the aggressive behavior of human epithelial ovarian cancer. Cancer Res. *65*, 3025–3029.
6. Kakar, S.S., Ratajczak, M.Z., Powell, K.S., Moghadamfalahi, M., Miller, D.M., Batra, S.K., and Singh, S.K. (2014). Withaferin a alone and in combination with cisplatin suppresses growth and metastasis of ovarian cancer by targeting putative cancer stem cells. PLoS One *9*, e107596.
7. Kim, D.K., Ham, M.H., Lee, S.Y., Shin, M.J., Kim, Y.E., Song, P., Suh, D.S., and Kim, J.H. (2020). CD166 promotes the cancer stem-like properties of primary epithelial ovarian cancer cells. BMB Rep. *53*, 622–627.
8. Cole, A.J., Fayomi, A.P., Anyaeche, V.I., Bai, S., and Buckanovich, R.J. (2020). An evolving paradigm of cancer stem cell hierarchies: therapeutic implications. Theranostics *10*, 3083–3098.
9. Huang, T., Song, X., Xu, D., Tiek, D., Goenka, A., Wu, B., Sastry, N., Hu, B., and Cheng, S.Y. (2020). Stem cell programs in cancer initiation, progression, and therapy resistance. Theranostics *10*, 8721–8743.
10. Bao, S., Wu, Q., McLendon, R.E., Hao, Y., Shi, Q., Hjelmeland, A.B., Dewhirst, M.W., Bigner, D.D., and Rich, J.N. (2006). Glioma stem cells promote radioresistance by preferential activation of the DNA damage response. Nature *444*, 756–760.
11. Venkatesha, V.A., Parsels, L.A., Parsels, J.D., Zhao, L., Zabludoff, S.D., Simeone, D.M., Maybaum, J., Lawrence, T.S., and Morgan, M.A. (2012). Sensitization of pancreatic cancer stem cells to gemcitabine by Chk1 inhibition. Neoplasia *14*, 519–525.
12. Masaki, T., Shiratori, Y., Rengifo, W., Igarashi, K., Yamagata, M., Kurokohchi, K., Uchida, N., Miyauchi, Y., Yoshiji, H., Watanabe, S., et al. (2003). Cyclins and cyclin-dependent kinases: comparative study of hepatocellular carcinoma versus cirrhosis. Hepatology *37*, 534–543.
13. Iorns, E., Lord, C.J., Grigoriadis, A., McDonald, S., Fenwick, K., Mackay, A., Mein, C.A., Natrajan, R., Savage, K., Tamber, N., et al. (2009). Integrated functional, gene expression and genomic analysis for the identification of cancer targets. PLoS One *4*, e5120.
14. Mir, S.E., De Witt Hamer, P.C., Krawczyk, P.M., Balaj, L., Claes, A., Niers, J.M., Van Tilborg, A.A.G., Zwinderman, A.H., Geerts, D., Kaspers, G.J.L., et al. (2010). In silico analysis of kinase expression identifies WEE1 as a gatekeeper against mitotic catastrophe in glioblastoma. Cancer Cell *18*, 244–257.
15. Magnussen, G.I., Holm, R., Emilsen, E., Rosnes, A.K.R., Slipicevic, A., and Flørenes, V.A. (2012). High expression of Wee1 is associated with poor disease-free survival in malignant melanoma: potential for targeted therapy. PLoS One *7*, e38254.
16. Slipicevic, A., Holth, A., Hellesylt, E., Tropé, C.G., Davidson, B., and Flørenes, V.A. (2014). Wee1 is a novel independent prognostic marker of poor survival in post-chemotherapy ovarian carcinoma effusions. Gynecol. Oncol. *135*, 118–124.
17. Dillon, M.T., Good, J.S., and Harrington, K.J. (2014). Selective targeting of the G2/M cell cycle checkpoint to improve the therapeutic index of radiotherapy. Clin. Oncol. *26*, 257–265.
18. Matheson, C.J., Venkataraman, S., Amani, V., Harris, P.S., Backos, D.S., Donson, A.M., Wempe, M.F., Foreman, N.K., Vibhakar, R., and Reigan, P. (2016). A WEE1 inhibitor analog of AZD1775 maintains synergy with cisplatin and demonstrates reduced single-agent cytotoxicity in medulloblastoma cells. ACS Chem. Biol. *11*, 2066–2067.
19. Lai, E.C. (2004). Predicting and validating microRNA targets. Genome Biol. *5*, 115.
20. Bertoli, G., Cava, C., and Castiglioni, I. (2015). MicroRNAs: new biomarkers for diagnosis, prognosis, therapy prediction and therapeutic tools for breast cancer. Theranostics *5*, 1122–1143.

21. Bartel, D.P. (2004). MicroRNAs: genomics, biogenesis, mechanism, and function. Cell *116*, 281–297.

22. Iorio, M.V., Ferracin, M., Liu, C.G., Veronese, A., Spizzo, R., Sabbioni, S., Magri, E., Pedriali, M., Fabbri, M., Campiglio, M., et al. (2005). MicroRNA gene expression deregulation in human breast cancer. Cancer Res. *65*, 7065–7070.

23. Akao, Y., Nakagawa, Y., and Naoe, T. (2007). MicroRNA-143 and -145 in colon cancer. DNA Cell Biol. *26*, 311–320.

24. Bloomston, M., Frankel, W.L., Petrocca, F., Volinia, S., Alder, H., Hagan, J.P., Liu, C.G., Bhatt, D., Taccioli, C., and Croce, C.M. (2007). MicroRNA expression patterns to differentiate pancreatic adenocarcinoma from normal pancreas and chronic pancreatitis. JAMA *297*, 1901–1908.

25. Iorio, M.V., Visone, R., Di Leva, G., Donati, V., Petrocca, F., Casalini, P., Taccioli, C., Volinia, S., Liu, C.G., Alder, H., et al. (2007). MicroRNA signatures in human ovarian cancer. Cancer Res. *67*, 8699–8707.

26. Yang, H., Kong, W., He, L., Zhao, J.J., O'Donnell, J.D., Wang, J., Wenham, R.M., Coppola, D., Kruk, P.A., Nicosia, S.V., and Cheng, J.Q. (2008). MicroRNA expression profiling in human ovarian cancer: miR-214 induces cell survival and cisplatin resistance by targeting PTEN. Cancer Res. *68*, 425–433.

27. Nguyen, M.T., Min, K.H., and Lee, W. (2020). MiR-183-5p induced by saturated fatty acids regulates the myogenic differentiation by directly targeting FHL1 in C2C12 myoblasts. BMB Rep. *53*, 605–610.

28. Chen, D., Zhang, Y., Wang, J., Chen, J., Yang, C., Cai, K., Wang, X., Shi, F., and Dou, J. (2013). MicroRNA-200c overexpression inhibits tumorigenicity and metastasis of CD117+CD44+ ovarian cancer stem cells by regulating epithelial-mesenchymal transition. J. Ovarian Res. *6*, 50.

29. Takahashi, R.U., Miyazaki, H., and Ochiya, T. (2014). The role of microRNAs in the regulation of cancer stem cells. Front. Genet. *4*, 295.

30. Jeong, J.Y., Kang, H., Kim, T.H., Kim, G., Heo, J.H., Kwon, A.Y., Kim, S., Jung, S.G., and An, H.J. (2017). MicroRNA-136 inhibits cancer stem cell activity and enhances the anti-tumor effect of paclitaxel against chemoresistant ovarian cancer cells by targeting Notch3. Cancer Lett. *386*, 168–178.

31. Jiang, W., Hu, J.W., He, X.R., Jin, W.L., and He, X.Y. (2021). Statins: a repurposed drug to fight cancer. J. Exp. Clin. Cancer Res. *40*, 241.

32. Jin, M.Z., and Jin, W.L. (2020). The updated landscape of tumor microenvironment and drug repurposing. Signal Transduct. Target. Ther. *5*, 166.

33. Matusewicz, L., Meissner, J., Toporkiewicz, M., and Sikorski, A.F. (2015). The effect of statins on cancer cells–review. Tumour Biol. *36*, 4889–4904.

34. Takwi, A.A.L., Li, Y., Becker Buscaglia, L.E., Zhang, J., Choudhury, S., Park, A.K., Liu, M., Young, K.H., Park, W.Y., Martin, R.C.G., and Li, Y. (2012). A statin-regulated microRNA represses human c-Myc expression and function. EMBO Mol. Med. *4*, 896–909.

35. Visvader, J.E., and Lindeman, G.J. (2012). Cancer stem cells: current status and evolving complexities. Cell Stem Cell *10*, 717–728.

36. Kenda Suster, N., and Virant-Klun, I. (2019). Presence and role of stem cells in ovarian cancer. World J. Stem Cells *11*, 383–397.

37. Curley, M.D., Therrien, V.A., Cummings, C.L., Sergent, P.A., Koulouris, C.R., Friel, A.M., Roberts, D.J., Seiden, M.V., Scadden, D.T., Rueda, B.R., and Foster, R. (2009). CD133 expression defines a tumor initiating cell population in primary human ovarian cancer. Stem Cell. *27*, 2875–2883.

38. Silva, I.A., Bai, S., McLean, K., Yang, K., Griffith, K., Thomas, D., Ginestier, C., Johnston, C., Kueck, A., Reynolds, R.K., et al. (2011). Aldehyde dehydrogenase in combination with CD133 defines angiogenic ovarian cancer stem cells that portend poor patient survival. Cancer Res. *71*, 3991–4001.

39. Shah, M.M., and Landen, C.N. (2014). Ovarian cancer stem cells: are they real and why are they important? Gynecol. Oncol. *132*, 483–489.

40. Ma, H., Lian, R., Wu, Z., Li, X., Yu, W., Shang, Y., and Guo, X. (2017). MiR-503 enhances the radiosensitivity of laryngeal carcinoma cells via the inhibition of WEE1. Tumour Biol. *39*, 1010428317706224.

41. Bhattacharya, A., Schmitz, U., Wolkenhauer, O., Schönherr, M., Raatz, Y., and Kunz, M. (2013). Regulation of cell cycle checkpoint kinase WEE1 by miR-195 in malignant melanoma. Oncogene *32*, 3175–3183.

42. Wang, L., Su, J., Zhao, Z., Hou, Y., Yin, X., Zheng, N., Zhou, X., Yan, J., Xia, J., and Wang, Z. (2017). MiR-26b reverses temozolomide resistance via targeting Wee1 in glioma cells. Cell Cycle *16*, 1954–1964.

43. Cha, S.Y., Choi, Y.H., Hwang, S., Jeong, J.Y., and An, H.J. (2017). Clinical impact of microRNAs associated with cancer stem cells as a prognostic factor in ovarian carcinoma. J. Cancer *8*, 3538–3547.

44. Kim, J., Kang, Y., Kojima, Y., Lighthouse, J.K., Hu, X., Aldred, M.A., McLean, D.L., Park, H., Comhair, S.A., Greif, D.M., et al. (2013). An endothelial apelin-FGF link mediated by miR-424 and miR-503 is disrupted in pulmonary arterial hypertension. Nat. Med. *19*, 74–82.

45. Lee, A., Papangeli, I., Park, Y., Jeong, H.N., Choi, J., Kang, H., Jo, H.N., Kim, J., and Chun, H.J. (2017). A PPARgamma-dependent miR-424/503-CD40 axis regulates inflammation mediated angiogenesis. Sci. Rep. *7*, 2528.

46. Dahiya, N., Sherman-Baust, C.A., Wang, T.L., Davidson, B., Shih, I.M., Zhang, Y., Wood, W., 3rd, Becker, K.G., and Morin, P.J. (2008). MicroRNA expression and identification of putative miRNA targets in ovarian cancer. PLoS One *3*, e2436.

47. Oneyama, C., Kito, Y., Asai, R., Ikeda, J.i., Yoshida, T., Okuzaki, D., Kokuda, R., Kakumoto, K., Takayama, K.i., Inoue, S., et al. (2013). MiR-424/503-mediated Rictor upregulation promotes tumor progression. PLoS One *8*, e80300.

48. Xu, Y.Y., Wu, H.J., Ma, H.D., Xu, L.P., Huo, Y., and Yin, L.R. (2013). MicroRNA-503 suppresses proliferation and cell-cycle progression of endometrioid endometrial cancer by negatively regulating cyclin D1. FEBS J. *280*, 3768–3779.

49. L'Espérance, S., Bachvarova, M., Tetu, B., Mes-Masson, A.M., and Bachvarov, D. (2008). Global gene expression analysis of early response to chemotherapy treatment in ovarian cancer spheroids. BMC Genom. *9*, 99.

50. Siu, M.K.Y., Wong, E.S.Y., Kong, D.S.H., Chan, H.Y., Jiang, L., Wong, O.G.W., Lam, E.W.F., Chan, K.K.L., Ngan, H.Y.S., Le, X.F., and Cheung, A.N. (2013). Stem cell transcription factor NANOG controls cell migration and invasion via dysregulation of E-cadherin and FoxJ1 and contributes to adverse clinical outcome in ovarian cancers. Oncogene *32*, 3500–3509.

51. Zhang, J., Espinoza, L.A., Kinders, R.J., Lawrence, S.M., Pfister, T.D., Zhou, M., Veenstra, T.D., Thorgeirsson, S.S., and Jessup, J.M. (2013). NANOG modulates stemness in human colorectal cancer. Oncogene *32*, 4397–4405.

52. McLean, D.L., Kim, J., Kang, Y., Shi, H., Atkins, G.B., Jain, M.K., and Chun, H.J. (2012). Apelin/APJ signaling is a critical regulator of statin effects in vascular endothelial cells–brief report. Arterioscler. Thromb. Vasc. Biol. *32*, 2640–2643.

53. Campbell, M.J., Esserman, L.J., Zhou, Y., Shoemaker, M., Lobo, M., Borman, E., Baehner, F., Kumar, A.S., Adduci, K., Marx, C., et al. (2006). Breast cancer growth prevention by statins. Cancer Res. *66*, 8707–8714.

54. Liu, H., Liang, S.L., Kumar, S., Weyman, C.M., Liu, W., and Zhou, A. (2009). Statins induce apoptosis in ovarian cancer cells through activation of JNK and enhancement of Bim expression. Cancer Chemother. Pharmacol. *63*, 997–1005.

55. Tsubaki, M., Takeda, T., Kino, T., Obata, N., Itoh, T., Imano, M., Mashimo, K., Fujiwara, D., Sakaguchi, K., Satou, T., and Nishida, S. (2015). Statins improve survival by inhibiting spontaneous metastasis and tumor growth in a mouse melanoma model. Am. J. Cancer Res. *5*, 3186–3197.

56. Lee, M.H., Cho, Y.S., and Han, Y.M. (2007). Simvastatin suppresses self-renewal of mouse embryonic stem cells by inhibiting RhoA geranylgeranylation. Stem Cell. *25*, 1654–1663.

57. Gauthaman, K., Manasi, N., and Bongso, A. (2009). Statins inhibit the growth of variant human embryonic stem cells and cancer cells in vitro but not normal human embryonic stem cells. Br. J. Pharmacol. *157*, 962–973.

58. Burgos-Ojeda, D., Rueda, B.R., and Buckanovich, R.J. (2012). Ovarian cancer stem cell markers: prognostic and therapeutic implications. Cancer Lett. *322*, 1–7.

59. Friedlander, M., Trimble, E., Tinker, A., Alberts, D., Avall-Lundqvist, E., Brady, M., Harter, P., Pignata, S., Pujade-Lauraine, E., Sehouli, J., et al. (2011). Clinical trials in recurrent ovarian cancer. Int. J. Gynecol. Cancer *21*, 771–775.

60. Mirza, M.R., Monk, B.J., Herrstedt, J., Oza, A.M., Mahner, S., Redondo, A., Fabbro, M., Ledermann, J.A., Lorusso, D., Vergote, I., et al. (2016). Niraparib maintenance therapy in platinum-sensitive, recurrent ovarian cancer. N. Engl. J. Med. *375*, 2154–2164.

61. Pujade-Lauraine, E., Ledermann, J.A., Selle, F., Gebski, V., Penson, R.T., Oza, A.M., Korach, J., Huzarski, T., Poveda, A., Pignata, S., et al. (2017). Olaparib tablets as maintenance therapy in patients with platinum-sensitive, relapsed ovarian cancer and a BRCA1/2 mutation (SOLO2/ENGOT-Ov21): a double-blind, randomised, placebo-controlled, phase 3 trial. Lancet Oncol. *18*, 1274–1284.

62. Ledermann, J., Harter, P., Gourley, C., Friedlander, M., Vergote, I., Rustin, G., Scott, C., Meier, W., Shapira-Frommer, R., Safra, T., et al. (2012). Olaparib maintenance therapy in platinum-sensitive relapsed ovarian cancer. N. Engl. J. Med. *366*, 1382–1392.

63. Coleman, R.L., Oza, A.M., Lorusso, D., Aghajanian, C., Oaknin, A., Dean, A., Colombo, N., Weberpals, J.I., Clamp, A., Scambia, G., et al. (2017). Rucaparib maintenance treatment for recurrent ovarian carcinoma after response to platinum therapy (ARIEL3): a randomised, double-blind, placebo-controlled, phase 3 trial. Lancet *390*, 1949–1961.

64. Zhang, S., Balch, C., Chan, M.W., Lai, H.C., Matei, D., Schilder, J.M., Yan, P.S., Huang, T.H.M., and Nephew, K.P. (2008). Identification and characterization of ovarian cancer-initiating cells from primary human tumors. Cancer Res. *68*, 4311–4320.

65. Murrow, L.M., Garimella, S.V., Jones, T.L., Caplen, N.J., and Lipkowitz, S. (2010). Identification of WEE1 as a potential molecular target in cancer cells by RNAi screening of the human tyrosine kinome. Breast Cancer Res. Treat. *122*, 347–357.

66. Lee, M., Nam, E.J., Kim, S.W., Kim, S., Kim, J.H., and Kim, Y.T. (2012). Prognostic impact of the cancer stem cell-related marker NANOG in ovarian serous carcinoma. Int. J. Gynecol. Cancer *22*, 1489–1496.

67. Egeland, E.V., Flatmark, K., Nesland, J.M., Florenes, V.A., Mælandsmo, G.M., and Boye, K. (2016). Expression and clinical significance of Wee1 in colorectal cancer. Tumour Biol. *37*, 12133–12140.

68. Kim, H.Y., Cho, Y., Kang, H., Yim, Y.S., Kim, S.J., Song, J., and Chun, K.H. (2016). Targeting the WEE1 kinase as a molecular targeted therapy for gastric cancer. Oncotarget *7*, 49902–49916.

69. Kreahling, J.M., Foroutan, P., Reed, D., Martinez, G., Razabdouski, T., Bui, M.M., Raghavan, M., Letson, D., Gillies, R.J., and Altiok, S. (2013). Wee1 inhibition by MK-1775 leads to tumor inhibition and enhances efficacy of gemcitabine in human sarcomas. PLoS One *8*, e57523.

70. Maugeri-Saccà, M., Bartucci, M., and De Maria, R. (2012). DNA damage repair pathways in cancer stem cells. Mol. Cancer Ther. *11*, 1627–1636.

71. Syljuåsen, R.G., Hasvold, G., Hauge, S., and Helland, Å. (2015). Targeting lung cancer through inhibition of checkpoint kinases. Front. Genet. *6*, 70.

72. Rajeshkumar, N.V., De Oliveira, E., Ottenhof, N., Watters, J., Brooks, D., Demuth, T., Shumway, S.D., Mizuarai, S., Hirai, H., Maitra, A., and Hidalgo, M. (2011). MK-1775, a potent Wee1 inhibitor, synergizes with gemcitabine to achieve tumor regressions, selectively in p53-deficient pancreatic cancer xenografts. Clin. Cancer Res. *17*, 2799–2806.

73. Hirai, H., Arai, T., Okada, M., Nishibata, T., Kobayashi, M., Sakai, N., Imagaki, K., Ohtani, J., Sakai, T., Yoshizumi, T., et al. (2010). MK-1775, a small molecule Wee1 inhibitor, enhances anti-tumor efficacy of various DNA-damaging agents, including 5-fluorouracil. Cancer Biol. Ther. *9*, 514–522.

74. Hirai, H., Iwasawa, Y., Okada, M., Arai, T., Nishibata, T., Kobayashi, M., Kimura, T., Kaneko, N., Ohtani, J., Yamanaka, K., et al. (2009). Small-molecule inhibition of Wee1 kinase by MK-1775 selectively sensitizes p53-deficient tumor cells to DNA-damaging agents. Mol. Cancer Ther. *8*, 2992–3000.

75. Mizuarai, S., Yamanaka, K., Itadani, H., Arai, T., Nishibata, T., Hirai, H., and Kotani, H. (2009). Discovery of gene expression-based pharmacodynamic biomarker for a p53 context-specific anti-tumor drug Wee1 inhibitor. Mol. Cancer *8*, 34.

76. Bridges, K.A., Hirai, H., Buser, C.A., Brooks, C., Liu, H., Buchholz, T.A., Molkentine, J.M., Mason, K.A., and Meyn, R.E. (2011). MK-1775, a novel Wee1 kinase inhibitor, radiosensitizes p53-defective human tumor cells. Clin. Cancer Res. *17*, 5638–5648.

77. Cancer Genome Atlas Research Network (2011). Integrated genomic analyses of ovarian carcinoma. Nature *474*, 609–615.

78. Oza, A.M., Estevez-Diz, M., Grischke, E.M., Hall, M., Marmé, F., Provencher, D., Uyar, D., Weberpals, J.I., Wenham, R.M., Laing, N., et al. (2020). A biomarker-enriched, randomized phase II trial of adavosertib (AZD1775) plus paclitaxel and carboplatin for women with platinum-sensitive TP53-mutant ovarian cancer. Clin. Cancer Res. *26*, 4767–4776.

79. Lheureux, S., Cristea, M.C., Bruce, J.P., Garg, S., Cabanero, M., Mantia-Smaldone, G., Olawaiye, A.B., Ellard, S.L., Weberpals, J.I., Wahner Hendrickson, A.E., et al. (2021). Adavosertib plus gemcitabine for platinum-resistant or platinum-refractory recurrent ovarian cancer: a double-blind, randomised, placebo-controlled, phase 2 trial. Lancet *397*, 281–292.

80. Coleman, R.L., Spirtos, N.M., Enserro, D., Herzog, T.J., Sabbatini, P., Armstrong, D.K., Kim, J.W., Park, S.Y., Kim, B.G., Nam, J.H., et al. (2019). Secondary surgical cytoreduction for recurrent ovarian cancer. N. Engl. J. Med. *381*, 1929–1939.

81. Pujade-Lauraine, E., Hilpert, F., Weber, B., Reuss, A., Poveda, A., Kristensen, G., Sorio, R., Vergote, I., Witteveen, P., Bamias, A., et al. (2014). Bevacizumab combined with chemotherapy for platinum-resistant recurrent ovarian cancer: the AURELIA open-label randomized phase III trial. J. Clin. Oncol. *32*, 1302–1308.

82. Mueller, S., Hashizume, R., Yang, X., Kolkowitz, I., Olow, A.K., Phillips, J., Smirnov, I., Tom, M.W., Prados, M.D., James, C.D., et al. (2014). Targeting Wee1 for the treatment of pediatric high-grade gliomas. Neuro Oncol. *16*, 352–360.

83. Li, Y., Guessous, F., Zhang, Y., Dipierro, C., Kefas, B., Johnson, E., Marcinkiewicz, L., Jiang, J., Yang, Y., Schmittgen, T.D., et al. (2009). MicroRNA-34a inhibits glioblastoma growth by targeting multiple oncogenes. Cancer Res. *69*, 7569–7576.

84. Liu, C., Kelnar, K., Liu, B., Chen, X., Calhoun-Davis, T., Li, H., Patrawala, L., Yan, H., Jeter, C., Honorio, S., et al. (2011). The microRNA miR-34a inhibits prostate cancer stem cells and metastasis by directly repressing CD44. Nat. Med. *17*, 211–215.

85. Liu, Q., Fu, H., Sun, F., Zhang, H., Tie, Y., Zhu, J., Xing, R., Sun, Z., and Zheng, X. (2008). miR-16 family induces cell cycle arrest by regulating multiple cell cycle genes. Nucleic Acids Res. *36*, 5391–5404.

86. Rissland, O.S., Hong, S.J., and Bartel, D.P. (2011). MicroRNA destabilization enables dynamic regulation of the miR-16 family in response to cell-cycle changes. Mol. Cell *43*, 993–1004.

87. Pouliot, L.M., Chen, Y.C., Bai, J., Guha, R., Martin, S.E., Gottesman, M.M., and Hall, M.D. (2012). Cisplatin sensitivity mediated by WEE1 and CHK1 is mediated by miR-155 and the miR-15 family. Cancer Res. *72*, 5945–5955.

88. Li, Q., Qiu, X.M., Li, Q.H., Wang, X.Y., Li, L., Xu, M., Dong, M., and Xiao, Y.B. (2015). MicroRNA-424 may function as a tumor suppressor in endometrial carcinoma cells by targeting E2F7. Oncol. Rep. *33*, 2354–2360.

89. Rodriguez-Barrueco, R., Nekritz, E.A., Bertucci, F., Yu, J., Sanchez-Garcia, F., Zeleke, T.Z., Gorbatenko, A., Birnbaum, D., Ezhkova, E., Cordon-Cardo, C., et al. (2017). miR-424(322)/503 is a breast cancer tumor suppressor whose loss promotes resistance to chemotherapy. Genes Dev. *31*, 553–566.

90. Xu, S., Tao, Z., Hai, B., Liang, H., Shi, Y., Wang, T., Song, W., Chen, Y., OuYang, J., Chen, J., et al. (2016). miR-424(322) reverses chemoresistance via T-cell immune response activation by blocking the PD-L1 immune checkpoint. Nat. Commun. *7*, 11406.

91. Lee, A., McLean, D., Choi, J., Kang, H., Chang, W., and Kim, J. (2014). Therapeutic implications of microRNAs in pulmonary arterial hypertension. BMB Rep. *47*, 311–317.

92. Pan, G., and Thomson, J.A. (2007). Nanog and transcriptional networks in embryonic stem cell pluripotency. Cell Res. *17*, 42–49.

93. Miyoshi, N., Ishii, H., Nagai, K.i., Hoshino, H., Mimori, K., Tanaka, F., Nagano, H., Sekimoto, M., Doki, Y., and Mori, M. (2010). Defined factors induce reprogramming of gastrointestinal cancer cells. Proc. Natl. Acad. Sci. USA *107*, 40–45.

94. Liu, S., Sun, J., Cai, B., Xi, X., Yang, L., Zhang, Z., Feng, Y., and Sun, Y. (2016). NANOG regulates epithelial-mesenchymal transition and chemoresistance through activation of the STAT3 pathway in epithelial ovarian cancer. Tumour Biol. *37*, 9671–9680.

95. Jeter, C.R., Liu, B., Liu, X., Chen, X., Liu, C., Calhoun-Davis, T., Repass, J., Zaehres, H., Shen, J.J., and Tang, D.G. (2011). NANOG promotes cancer stem cell characteristics and prostate cancer resistance to androgen deprivation. Oncogene *30*, 3833–3845.

96. Noh, K.H., Kim, B.W., Song, K.H., Cho, H., Lee, Y.H., Kim, J.H., Chung, J.Y., Kim, J.H., Hewitt, S.M., Seong, S.Y., et al. (2012). Nanog signaling in cancer promotes stem-like phenotype and immune evasion. J. Clin. Invest. *122*, 4077–4093.

97. Liang, J., Wan, M., Zhang, Y., Gu, P., Xin, H., Jung, S.Y., Qin, J., Wong, J., Cooney, A.J., Liu, D., and Songyang, Z. (2008). Nanog and Oct4 associate with unique transcriptional repression complexes in embryonic stem cells. Nat. Cell Biol. *10*, 731–739.

98. Torres, J., and Watt, F.M. (2008). Nanog maintains pluripotency of mouse embryonic stem cells by inhibiting NFkappaB and cooperating with Stat3. Nat. Cell Biol. *10*, 194–201.

99. Li, Q., Lex, R.K., Chung, H., Giovanetti, S.M., Ji, Z., Ji, H., Person, M.D., Kim, J., and Vokes, S.A. (2016). The pluripotency factor NANOG binds to GLI proteins and represses hedgehog-mediated transcription. J. Biol. Chem. *291*, 7171–7182.

100. Boudreau, D.M., Yu, O., and Johnson, J. (2010). Statin use and cancer risk: a comprehensive review. Expert Opin. Drug Saf. *9*, 603–621.

101. Kwan, M.L., Habel, L.A., Flick, E.D., Quesenberry, C.P., and Caan, B. (2008). Post-diagnosis statin use and breast cancer recurrence in a prospective cohort study of early stage breast cancer survivors. Breast Cancer Res. Treat. *109*, 573–579.

102. Ahern, T.P., Pedersen, L., Tarp, M., Cronin-Fenton, D.P., Garne, J.P., Silliman, R.A., Sørensen, H.T., and Lash, T.L. (2011). Statin prescriptions and breast cancer recurrence risk: a Danish nationwide prospective cohort study. J. Natl. Cancer Inst. *103*, 1461–1468.

103. Condello, S., Morgan, C.A., Nagdas, S., Cao, L., Turek, J., Hurley, T.D., and Matei, D. (2015). beta-Catenin-regulated ALDH1A1 is a target in ovarian cancer spheroids. Oncogene *34*, 2297–2308.

104. Condello, S., Sima, L., Ivan, C., Cardenas, H., Schiltz, G., Mishra, R.K., and Matei, D. (2018). Tissue tranglutaminase regulates interactions between ovarian cancer stem cells and the tumor niche. Cancer Res. *78*, 2990–3001.

OMTN, Volume *29*

Supplemental information

MicroRNA-dependent inhibition of WEE1 controls cancer stem-like characteristics and malignant behavior in ovarian cancer

Jin Gu Cho, Sung-wook Kim, Aram Lee, Ha-neul Jeong, Eunsik Yun, Jihea Choi, Su Jin Jeong, Woochul Chang, Sumin Oh, Kyung Hyun Yoo, Jung Bok Lee, Sukjoon Yoon, Myeong-Sok Lee, Jong Hoon Park, Min Hyung Jung, So-Woon Kim, Ki Hyung Kim, Dong Soo Suh, Kyung Un Choi, Jungmin Choi, Jongmin Kim, and Byung Su Kwon

Supplementary Material

Materials and methods

Lentivirus production and generation of stable cells

Lenti-miR microRNA precursors for hsa-miR-424 and hsa-miR-503 (System Biosciences, Palo Alto, CA, USA) were used along with a GFP control lentivirus. The Lenti-X HTX Packaging System (Clontech, Mountain View, CA, USA) was used to generate the lentiviral particles. HEK293T cells were transfected with lentiviral constructs using the FuGene HD Transfection Reagent (Promega, Madison, WI, USA) and incubated for 24 h. The viral particles in supernatants were harvested on ice, and the titer was measured using a qPCR Lentivirus Titration Kit (Applied Biological Materials, Richmond, BC, Canada). To generate the miR-424/503 overexpression stable cell line, SKOV3 cells were transfected with lenti-miR miRNA precursors for hsa-miR-424/503 and control, after which they were selected with puromycin (1 μg/mL, Sigma- Aldrich, St. Louis, MO, USA). The stable overexpression of miR-424/503 was confirmed through quantitative real-time PCR and fluorescence microscopy.

Proliferation assay

Cells were seeded at 1×10^4 cells/well in 96-well plates and treated with atorvastatin for 24 h in the monolayer state, and the spheroids were treated with atorvastatin in poly-HEMA-coated 96-well plates for 3 days. Cytotoxicity was measured using the EZ-Cytox WST kit (Daeil Lab Service, Seoul, Korea) according to the manufacturer's instructions. After adding 10 μL of the WST-1 reagent, the cells were incubated for 30 min, following which the absorbance was measured at 450 nm using a microplate reader.

Luciferase reporter assay

The pLightSwitch_WEE1 3′ UTR vector including Human WEE1 3′ UTR was purchased from SwitchGear Genomics (Carlsbad, CA, USA). The seed sequence of the WEE1 gene, TGCTGCTA, was mutated to CGCCGCCA using the Muta-DirectTM Site Directed Mutagenesis Kit (iNtRON Biotechnology, Seongnam, Korea). SKOV3 cells were transfected with the luciferase reporter constructs (containing either the wild-type or mutant WEE1 3′ UTR) and miRNAs (either pre-miR-424/503 mimics or negative control) using Lipofectamine 2000 (Invitrogen). After incubation for 48 h, the cells were lysed using a passive lysis buffer, and luciferase activity was measured using the Dual Luciferase® Reporter Assay System (Promega). The human miR-424/503 promoter luciferase construct was previously described.[1, 2] The SKOV3 cells were transfected with miR-424/503 promoter luciferase construct, renilla luciferase, and NANOG constructs. Luciferase activity was quantified using the Dual-Luciferase Reporter Assay kit (Promega).

Migration assay

Cells were infected with lentiviral miR-424/503 and control GFP and incubated for 24 h. The infected cells were seeded at 2×10^5 cells/well in 12-well plates. The cells were scratched using a 200 μL pipette tip and incubated for 12 h in a starvation medium supplemented with 1% FBS. The cells were observed under an optical microscope at 40× magnification. The differences in the width of the gaps were calculated using the ImageJ software.

Colony formation assay

For the colony formation assay, 1×10^3 cells were plated in 6-well plates with complete medium to culture for 2 weeks after transfection with miRNAs. After growth in the plates for 14 days, the colonies were washed with PBS buffer and stained with 0.5% crystal violet in 20% methanol

for 20 min, after which the number of colonies was determined.

In vitro limiting dilution assay

Cells were seeded in poly-HEMA coated 96-well plates at various concentrations (1–128 cells/well). DMSO and 10 μM atorvastatin were administered simultaneously with seeding. After incubation for 7 days, the number of wells without spheres at each seeding density was determined and plotted against the number of cells/well.

Flow cytometry analysis

For the analysis of individual cells, the spheroids were dissociated using a Cell Dissociation Buffer (Thermo Scientific). The number of cells exhibiting aldehyde dehydrogenase (ALDH) enzyme activity was measured using an Aldefluor kit (Stem Cell Technologies, Vancouver, Canada). For this, 1×10^6 cells were suspended in 1 mL of the ALDEFLOR assay buffer containing the ALDH substrate (BODIPY aminoacetaldehyde), and as negative controls, aliquots of each sample were treated with diethylaminobenzaldehyde, a specific ALDH inhibitor. Samples were incubated for 45 min at 37ºC before analysis. To detect the CSC marker CD133, the cells were labeled with the CD133-PE antibody (1:300, 130-080-801, Miltenyi Biotec, Bergisch Gladbach, Germany) for 1 h in PBS containing 0.1% BSA. All assessments were performed using an FACS CantoII flow cytometer, and the data were analyzed using the FlowJo software.

Bioinformatics analysis

Public data was downloaded from GEO (https://www.ncbi.nlm.nih.gov/geo/) and re-analyzed to validate inverse and/or positive correlation patterns between the expression levels of genes (GSE30161). Correlation was confirmed with correlation coefficiency values and linear

regression. The correlation coefficient between variables was calculated by the Pearson` method of cor() function and the linear regression model was calculated with the lm() function in R language. Progressive-free survival (PFS) and overall survival (OS) analyses were performed using Kaplan-Meier Plotter (Lanczky A, Gyorffy B: Web-Based Survival Analysis Tool Tailored for Medical Research (KMplot).[3]

Supplementary Table

Table S1. List of antibodies used

Application	Antibody	Raised	Manufacturer	Catalog number	Dilution
WB	AGO2	Mouse	Abcam	ab27113	1:1000
WB	Caspase 3	Rabbit	Cell Signaling	#9662	1:1000
WB	GAPDH	Rabbit	Cell Signaling	#2118	1:4000
WB	NANOG	Rabbit	Cell Signaling	#4903	1:1000
WB	WEE1	Rabbit	Cell Signaling	#4936	1:1000
WB	Anti-rabbit IgG-HRP	Goat	Cell Signaling	#7074	1:4000
WB	Anti-mouse IgG-HRP	Goat	Thermo Fisher Scientific	31430	1:4000
FACS	CD133-PE	Mouse	Miltenyi Biotec	130-080-801	1:300
IHC	WEE1	Mouse	Santa Cruz Biotechnology	sc-5285	1:100
IF	DAPI		Thermo Fisher Scientific	62248	1:1000
IF	ALDH1-Alexa 594		Santa Cruz Biotechnology	sc-166362 AF594	1:100
IF	WEE1-Alexa 488		Santa Cruz Biotechnology	sc-5285 AF488	1:100

Supplementary Figures

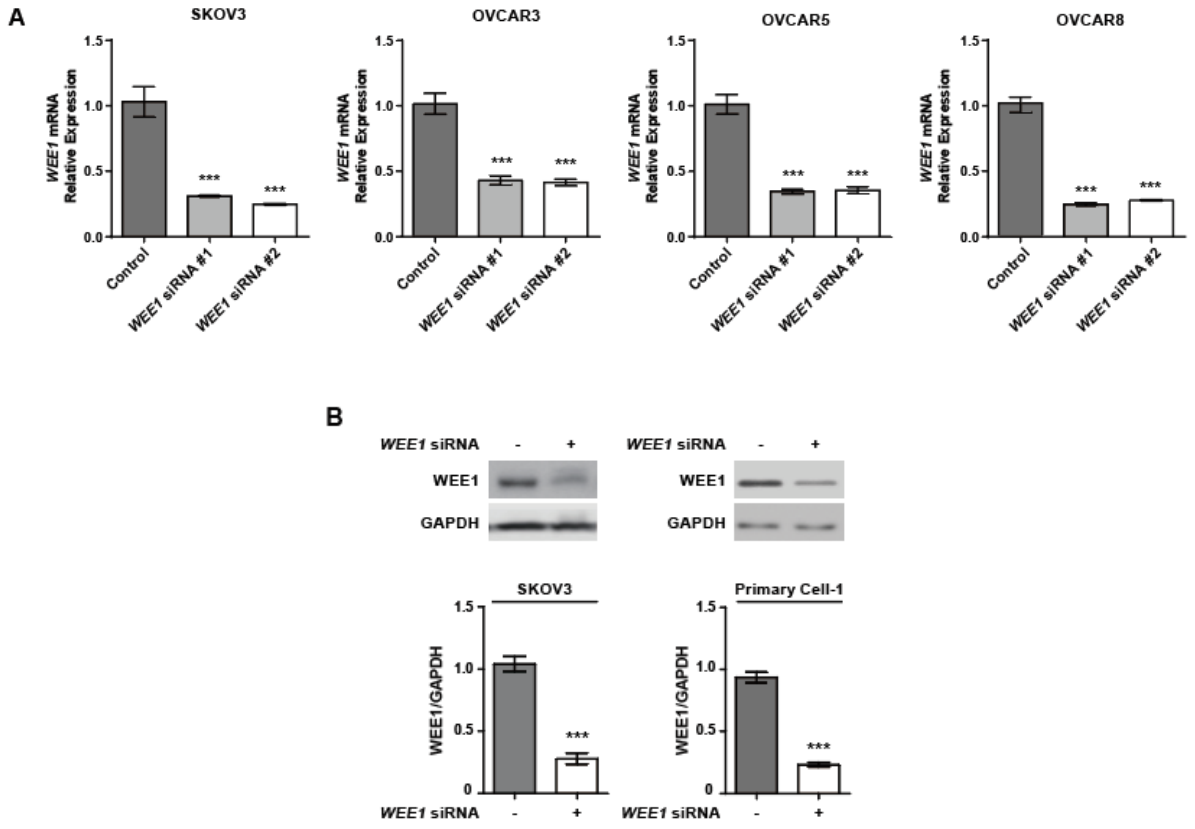

Figure S1. Knockdown efficacy of WEE1 in ovarian cancer cells.

(A) qRT-PCR showing *WEE1* mRNA expression after transfection with two distinct siRNAs (B) Western blot showing WEE1 protein levels. ***$P < 0.001$ by Student's *t*-test.

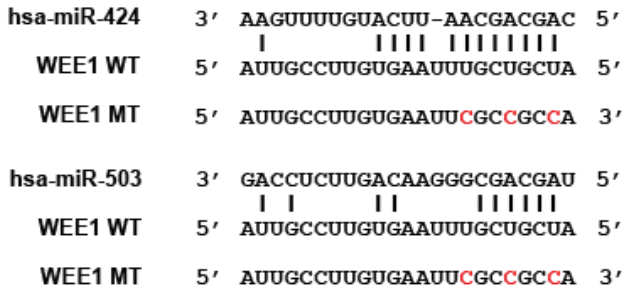

Figure S2. Predicted sequences of the WEE1 3′-UTR targeted by miR-424 and miR-503 and mutated sequences for disruption of the miR-424 and miR-503 binding sequence.

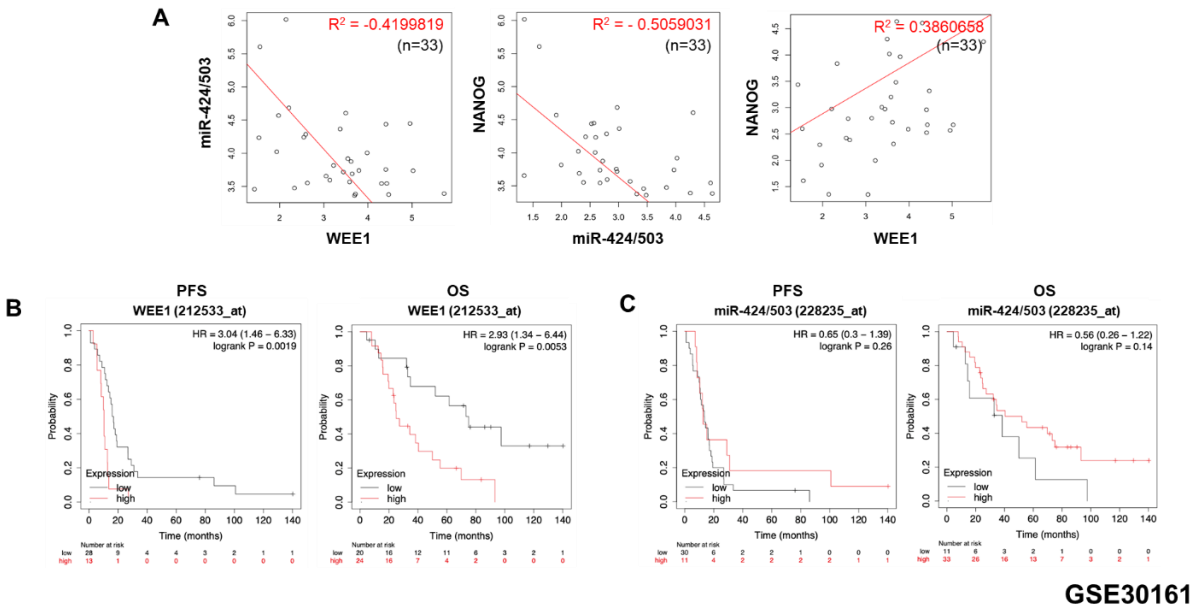

Figure S3. Relationship between miR-424/520, WEE1, and NANOG and patient outcomes in the GSE30161 dataset.

(A) Correlation analysis on the expression of miR-424/503, WEE1 and NANOG in patients with ovarian cancer. As shown, miR-424/503 had a strong inverse correlation with both WEE1 and NANOG, whereas WEE1 and NANOG had a significant positive correlation. (B) Kaplan-Meier survival curves for high and low expression of WEE1 in patients with ovarian cancer. WEE1 high expression is associated with poor PFS and OS survival. (C) Kaplan-Meier survival curves of the high and low expression of miR-424/503 in patients with ovarian cancer. Higher level of miR-424 and miR-503 expression revealed a trend in favor of PFS and OS survival. PFS; Progression-free survival, OS; Overall survival.

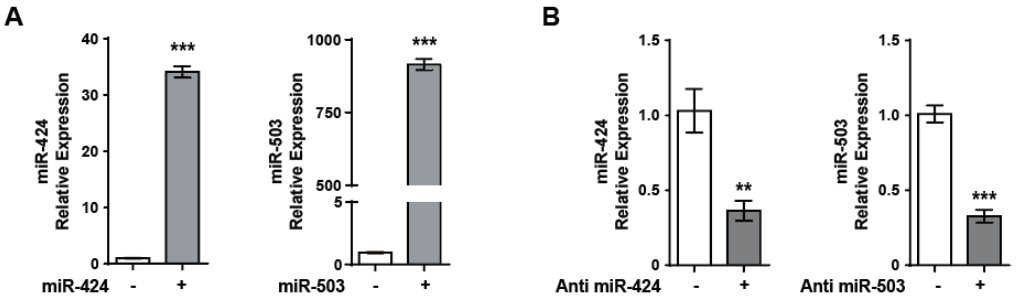

Figure S4. Overexpression knockdown efficacy of miR-424/503 in ovarian cancer cells.

(A) Levels of miRNA achieved with overexpression in ovarian cancer cells. (B) Levels of miRNA achieved with knockdown in ovarian cancer cells. $^{**}P < 0.01$, $^{***}P < 0.001$ by Student's *t*-test.

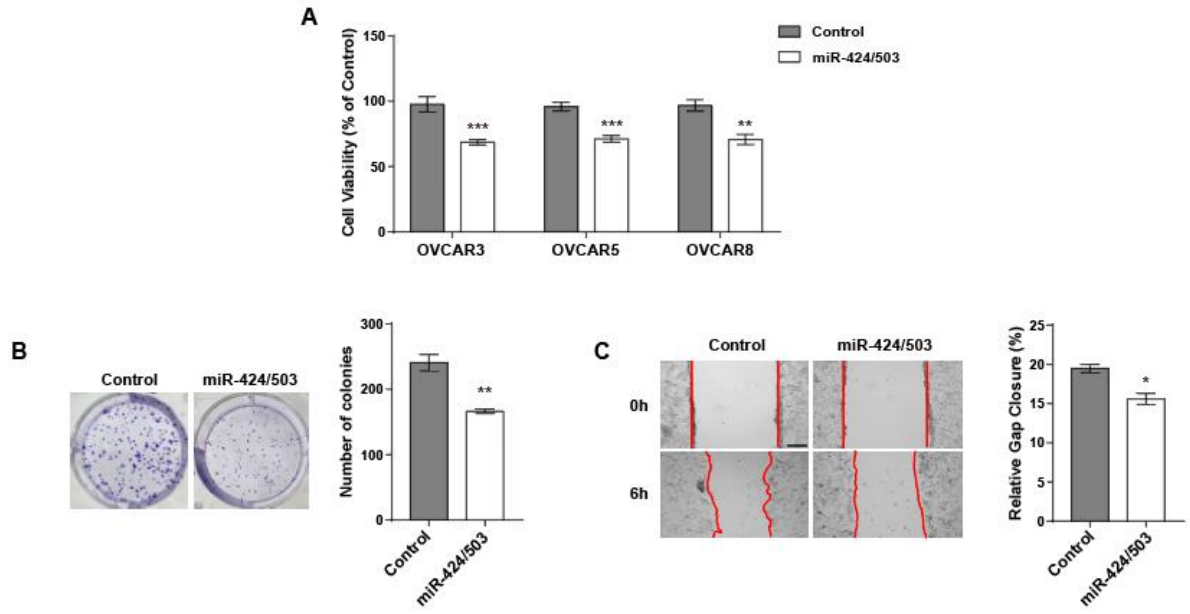

Figure S5. Cell viability, migration and colony assay after the overexpression of miR-424 and miR-503 in adherent OVCAR3, OVCAR5 and OVCAR8 cells.

(A) Cell viability after the overexpression of miR-424 and miR-503 in adherent OVCAR3, OVCAR5 and OVCAR8 cells. (B) Colony formation was determined using crystal violet staining 14 days after the miR-424 and miR-503 overexpression in adherent OVCAR8 cells. (C) Migration assay after miR-424/503 overexpression in adherent OVCAR8 cells. Scale bar: 200 μm. **P* < 0.05, ***P* < 0.01, ****P* < 0.001 by Student's *t*-test.

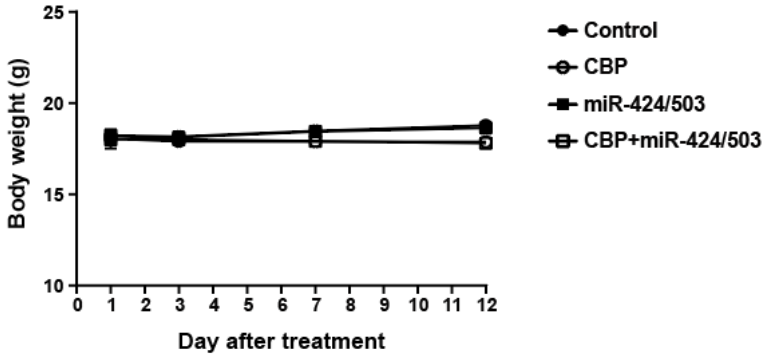

Figure S6. The effect of CBP and miR-424/503 on the body weight of SKOV3 xenograft mice.

No significant changes were observed in body weights among the different groups.

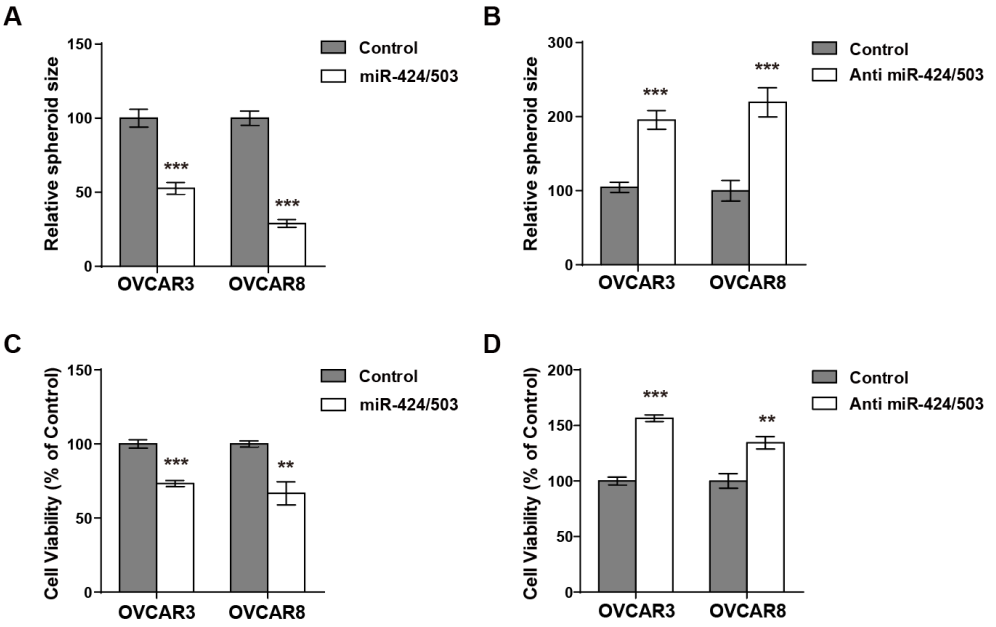

Figure S7. Cancer stem cell-like properties following the overexpression or inhibition of miR-424/503 in OVCAR3 and OVCAR8 cells.

The sizes of the spheroids after the overexpression (A) or inhibition (B) of miR-424/503 in OVCAR3 and OVCAR8 cells. Cell viability after the overexpression (C) or inhibition (D) of miR-424/503 in OVCAR3 and OVCAR8 spheroids. $^{**}P < 0.01$, $^{***}P < 0.001$ by Student's *t*-test.

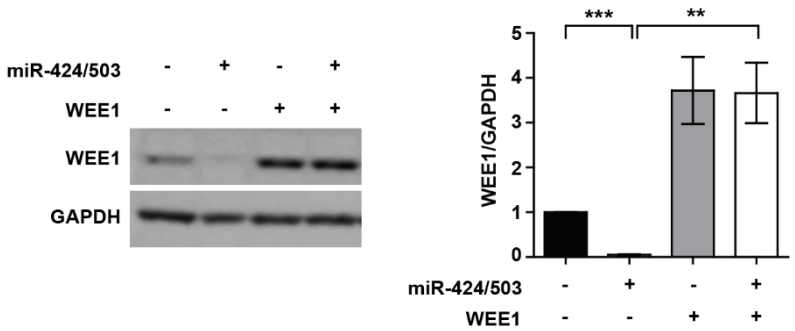

Figure S8. WEE1 protein expression levels after concurrent miR-424/503 and WEE1 overexpression. $^{**}P < 0.01$, $^{***}P < 0.001$ compared to controls by unpaired two-tailed Student's *t-test* or one-way ANOVA with Bonferroni's multiple comparison test. Error bars, standard error of the mean.

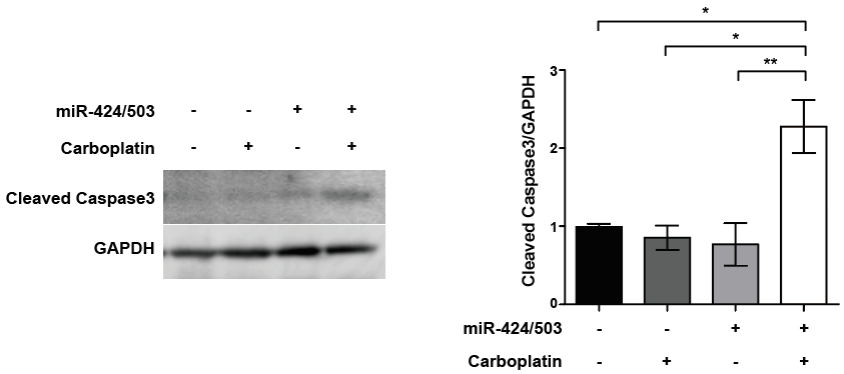

Figure S9. Increased caspase-3 cleavage in response to miR-424/503 overexpression upon carboplatin treatment of SKOV3 spheroids.

*P < 0.05, **P < 0.01 by one-way ANOVA, with Bonferroni *post-hoc* test.

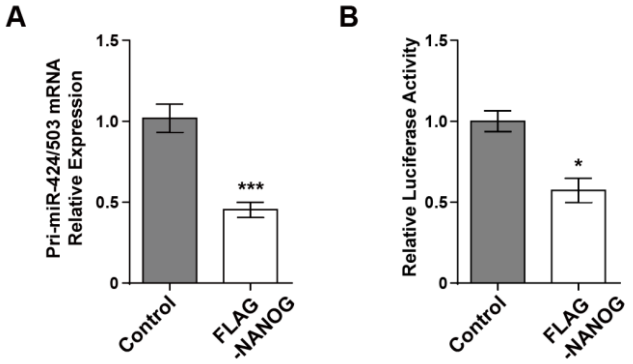

Figure S10. NANOG regulates miR-424/503 expression.

(A) Pri-forms of miR-424 and miR-503 expression in response to NANOG overexpression. (B) Relative luciferase activity of SKOV3 cells co-transfected with miR-424/503 promoter luciferase construct and NANOG. *P < 0.05, ***P < 0.001 by Student's t-test.

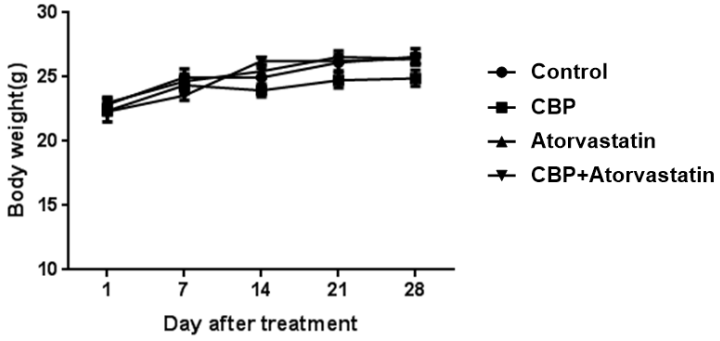

Figure S11. The effect of CBP and atorvastatin on the body weight of SKOV3 xenograft mice.

No significant changes were observed in body weights among the different groups.

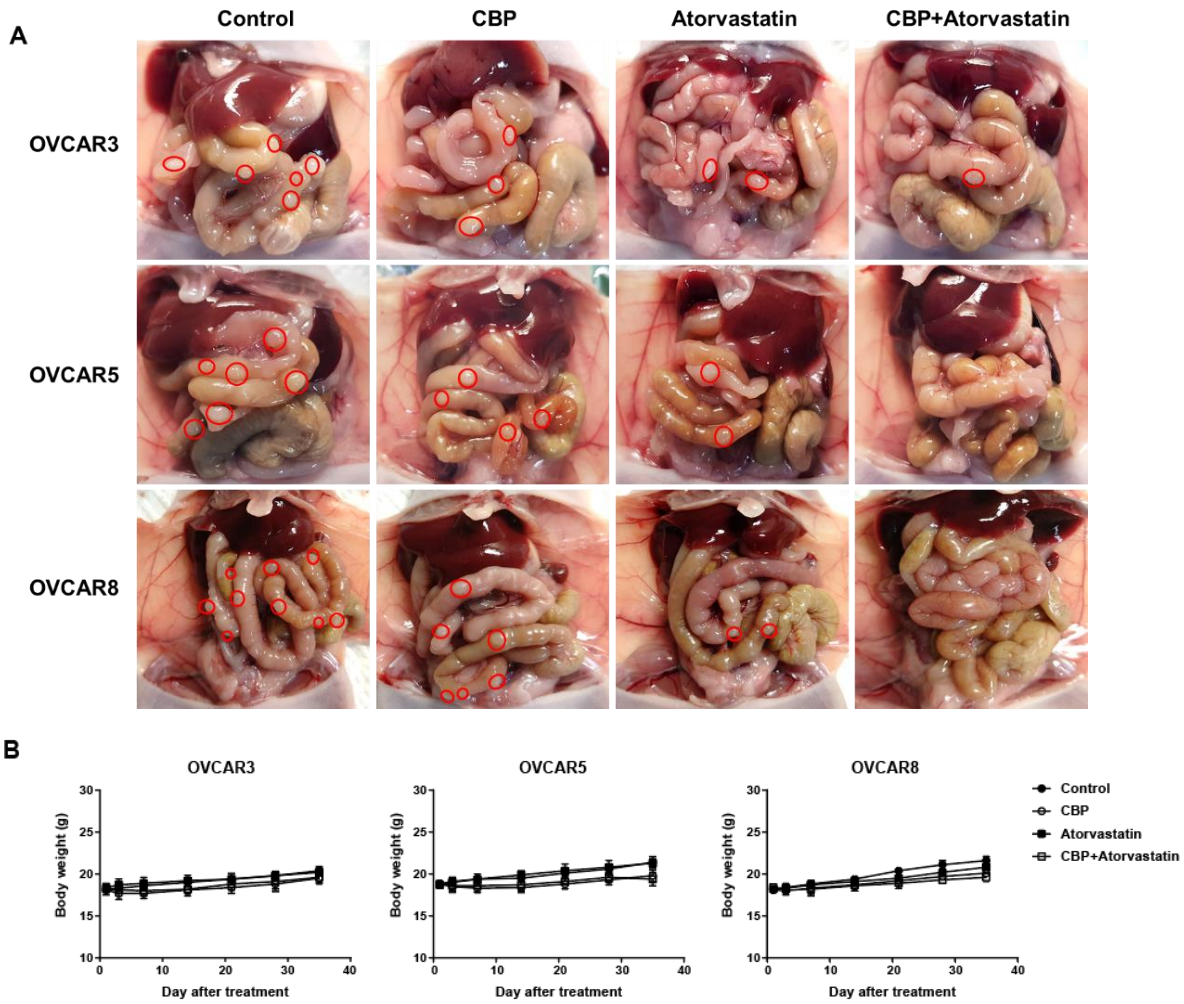

Figure S12. Combined treatment with carboplatin and atorvastatin inhibited ovarian cancer in the OVCAR3, OVCAR5 and OVCAR8 xenograft mouse model.

(A) Representative images of the peritoneal cavities of mice showing reduction in peritoneal tumors in the CBP, atorvastatin, and atorvastatin/CBP groups compared to that in the control group. (B) The effect of CBP and atorvastatin on the body weight of OVCAR3, OVCAR5 and OVCAR8 xenograft mice. $*P < 0.05$, $**P < 0.01$, $***P < 0.001$ by one-way analysis of variance (ANOVA), with Bonferroni *post-hoc* test.

References

1. Kim, J, Kang, Y, Kojima, Y, Lighthouse, JK, Hu, X, Aldred, MA, McLean, DL, Park, H, Comhair, SA, Greif, DM, *et al.* (2013). An endothelial apelin-FGF link mediated by miR-424 and miR-503 is disrupted in pulmonary arterial hypertension. *Nat Med* **19**: 74-82.
2. Lee, A, Papangeli, I, Park, Y, Jeong, HN, Choi, J, Kang, H, Jo, HN, Kim, J, and Chun, HJ (2017). A PPARgamma-dependent miR-424/503-CD40 axis regulates inflammation mediated angiogenesis. *Sci Rep* **7**: 2528.
3. Lanczky, A, and Gyorffy, B (2021). Web-Based Survival Analysis Tool Tailored for Medical Research (KMplot): Development and Implementation. *J Med Internet Res* **23**: e27633.